NASA CONTRACTOR REPORT

NASA CR-1398

LABORATORY EXPERIMENTS ON REVERTED RUBBER FRICTION

by G. H. Nybakken, R. J. Staples, and S. K. Clark

Prepared by
UNIVERSITY OF MICHIGAN
Ann Arbor, Mich.
for

NATIONAL AERONAUTICS AND SPACE ADMINISTRATION • WASHINGTON, D. C. • AUGUST 1969

LABORATORY EXPERIMENTS ON REVERTED RUBBER FRICTION

By G. H. Nybakken, R. J. Staples, and S. K. Clark

Issued by Originator as Technical Report No. 7

Prepared under Grant No. NGR-23-005-010 by
UNIVERSITY OF MICHIGAN
Ann Arbor, Mich.

for

NATIONAL AERONAUTICS AND SPACE ADMINISTRATION

For sale by the Clearinghouse for Federal Scientific and Technical Information
Springfield, Virginia 22151 – CFSTI price $3.00

ABSTRACT

LABORATORY EXPERIMENTS ON REVERTED RUBBER FRICTION

Laboratory experiments were carried out to explain the mechanism of "reverted rubber" skidding as has been observed on aircraft tires. It was determined that surface heat generation is the cause of this rubber degradation, and that such "reverted rubber" exhibits remarkably low friction coefficients on wet surfaces, at all speeds, compared to unreverted rubber on dry surfaces. The process of "reverted rubber" sliding can take place at ambient temperatures, and is not dependent on the simultaneous presence of heat. It is believed to be caused by a thin water film between the soft "reverted" rubber and the rigid roadway.

TABLE OF CONTENTS

LIST OF ILLUSTRATIONS

LIST OF ILLUSTRATIONS (Concluded)

I. INTRODUCTION

Since about 1950 it has been realized that a significant number of aircraft landing accidents can be attributed to loss of braking or frictional capability after making contact with the runway. A concerted research effort has been underway for some years to explain the mechanisms involved in these cases of loss of braking. Some of the phenomena which have been identified are:

(a) Tire hydroplaning

(b) Viscous hydroplaning

(c) "Reverted rubber" skid

While the first two effects have been studied extensively, and are quite well understood, the "reverted rubber" skid has been the object of considerable speculation but little actual experiment. This report represents a contribution to the understanding of the "reverted rubber" problem by means of selected laboratory tests, which allow environmental conditions to be closely controlled.

II. SUMMARY

A sequence of controlled laboratory experiments was carried out with a view to explaining the mechanism of "reverted rubber" skidding, as observed on some aircraft tires. The primary results are listed below:

(a) The degradation of an aircraft tire tread surface to a soft sticky rubber, as commonly observed on tires which have been in "reverted rubber" skid, is caused by high surface temperature, of the order of 400°F to 600°F.

(b) Once rubber has become "reverted" by the presence of heat, an extremely low friction coefficient is observed on almost any smooth wetted surface.

(c) The low friction coefficient of reverted rubber can exist at room temperature with cool water.

(d) There is absolutely no evidence of steam in the contact area of a "reverted rubber" specimen exhibiting very low friction coefficient, since this process can take place at room temperature.

(e) The presence of low friction coefficients is not strongly influenced by most other operating variables such as velocity of sliding, contact pressure or liquid viscosity.

(f) Low friction coefficients can exist down to very low sliding speeds, say 5 or 10 knots.

(g) All of the grades of rubber tested here showed clear reversion tendencies at the temperatures previously listed. However, natural rubber seems to be most precipitously affected.

(h) The presence of low friction coefficients is seen most markedly on smooth wet surfaces. However, it is strongly suspected that such low friction requires an increasingly thick film of "reverted" rubber as the surfact roughness increases, and that such a film of rubber on aircraft tires would allow low friction values on normal runway surfaces.

III. MECHANICS OF THE REVERTED RUBBER SKID

In recent years aircraft skidding accidents have taken place under conditions thought to be impossible for conventional tire hydroplaning. These skidding accidents occurred on smooth, wet or puddled runways and were accompanied by a loss of braking down to speeds of 5-8 knots. Afterward the tires of the aircraft exhibited a characteristic patch of sticky, soft rubber on the tread. This patch of rubber was called "reverted" rubber because it appeared to have been reverted back to its unvulcanized, uncured state. Because the loss of braking friction occurred down to speeds well below those thought to be minimum for tire hydroplaning, this loss of friction was believed to be connected with the patch or patches of "reverted" rubber. White streaks of clean runway usually resulted from these "reverted" rubber aircraft skids.

Later on rubber chemists pointed out that soft sticky rubber may be the result of excessive heat. Along this line, Obertop[1] has suggested that low friction developed in wet skids may be the result of steam developed in the tire footprint. Applying this theory to reverted rubber skids, Horne et al.,[2] theorized that the soft sticky rubber could form a seal around the edge of the contact patch which would contain high pressure super-heated steam under the contact patch. This steam pressure would tend to lift the tire away from the pavement surface, and thus reduce traction on wet surfaces. The white streaks would be clean pavement cleared of contaminants by high pressure super-heated steam. A preliminary examination by Horne et al., in Ref. 2 led them to state

this theory, "Thus these initial results based on limited data indicate that reverted rubber may form and possibly provide better sealing around the periphery of the footprint than normal rubber, thus allowing a very thin film of water to be trapped in the footprint, heated up, and to possibly change state into steam as predicted by Obertop."

While the steam theory provides one possible explanation for the skidding accidents which have been observed, it is also possible that liquid films of various types could form in a particularly tenacious way with reverted rubber, in such a fashion as to give a slider bearing effect. The sequence of events leading to aircraft skidding could begin with a momentary locking of brakes, which could cause a sudden surface temperature rise in the sliding contact patch. The rubber in the contact patch could become "reverted," or soft and sticky, due to the heat. Following this, the tire could then slide over wetted surfaces with very low friction coefficient provided that liquid film pressures were sufficient to distort the now soft and sticky tread rubber in the neighborhood of asperity tips, so that no asperities actually broke through the liquid film to make direct contact with the rubber. Such a process would be a slider bearing type of motion, where now the slider is flexible and conforming.

These two theories represent fundamentally different ways of looking at the mechanics of reverted rubber skid. All of the laboratory evidence accumulated so far seems to favor the second theory, that of the flexible slider bearing, although on the basis of the limited data available we cannot rule out the presence of heat and steam in aircraft operating accidents.

IV. EXPERIMENTAL RESULTS

A. GENERAL SUMMARY OF EXPERIMENTS

Early laboratory experiments concentrated on attempting to cause reversion in test samples of rubber by sliding them at high velocities over relatively rough surfaces, such as fine emery cloth or concrete. These efforts were all quite unsuccessful, although a number of different attempts were made.

The first positive information came when an inflated natural rubber tube specimen was bent around a circular holder to form a shape roughly similar to a torus, as shown in Figure 1.

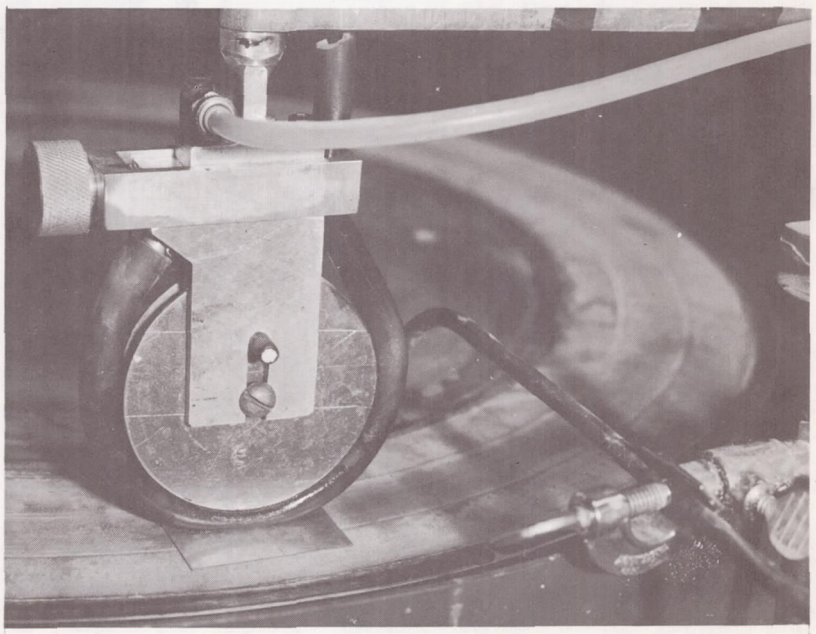

Figure 1. Tubing used as a model of a tire.

This specimen was then pressed against a rotating disc, similar to a record player, so that sliding velocities of the order of 20-50 mph were obtained. While rubber reversion could not be obtained by sliding, it was observed that

heating the tubing with a Bunsen burner produced a soft, sticky rubber surface similar to that observed in "reverted rubber" skidding accidents. After cooling, the treated tubing was tested on smooth wet surface. The friction values obtained were extremely low compared to values for untreated tubing tested under the same conditions. This large friction difference between untreated and treated tubing occurred on wet surfaces of smooth concrete, aluminum and epoxy-coated aluminum. While the tubing experiments are valuable, the inflation pressures, and hence contact pressures, are quite limited by the lack of strength and stiffness of the tubing. Reinforced tubing of this type was not readily available, and it was decided to use other specimen geometries having more design flexibility.

In an attempt to simulate the high contact pressures which exist between the tire tread and the runway, it was decided to use small solid rubber specimens cut from typical aircraft tire treads. These small rubber specimens were bonded to a larger steel mounting plate, as shown in Figure 2, which could in turn be heavily loaded. Prior to testing, the rubber specimens were heated by contact with a hot metal block of known temperature. After cooling, the specimens were run on a rotating, wet anodized aluminum surface. Temperature treatments of 500°F to 600°F again gave extremely low friction values when compared to untreated rubber friction values for the same test conditions. Since this temperature treatment alone gave the surface the characteristics of reverted rubber alone with low friction values, rubber treated in this way was given extensive testing with varying parameters of pressure, velocity, lubricant viscosity, temperature treatment and sample geometry. The details of such testing,

Detail of Sample Holders and Typical Samples

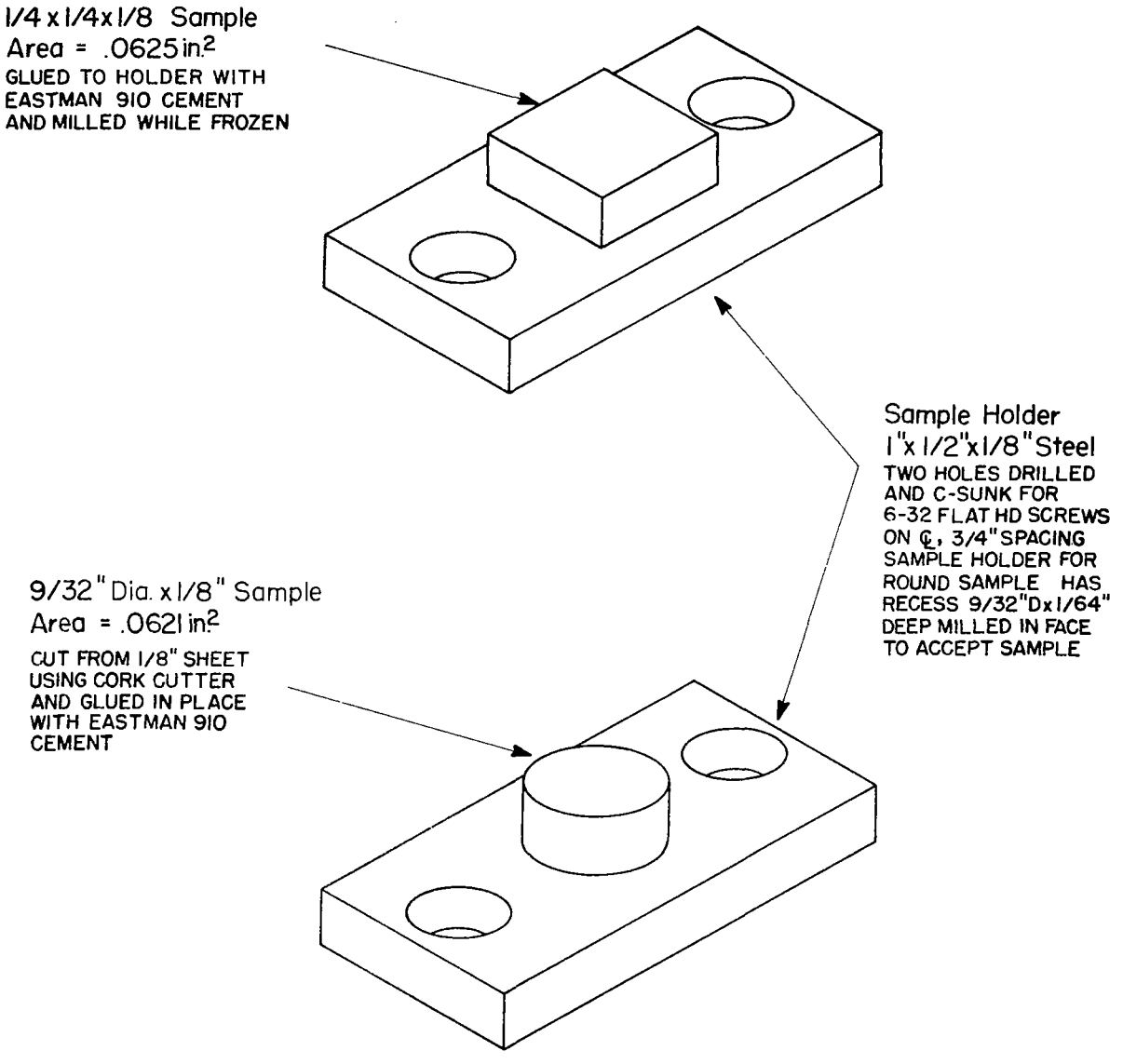

Figure 2. Specimen configuration for cut or machined rubber surfaces.

and the results, are presented in the following sections.

B. TEST APPARATUS

The laboratory apparatus used in the friction testing consisted of a rotating turntable faced with the friction surface and a hinged arm carrying the rubber sample. Figures 3, 4, and 5 show the most important features of this device, while Figure 6 is a drawing of it. The vertical sample holder is mounted below the narrow transducer section, where strain gages are used on the fore and aft sides of a beam to measure bending. Transducer output is converted directly into a drag force by means of previous calibration. Directly above the transducer is the dead weight system, used to provide normal load. The sample holder has a fore-aft adjustment to insure that this normal load acts directly through the center of the rubber sample. The counterweight at

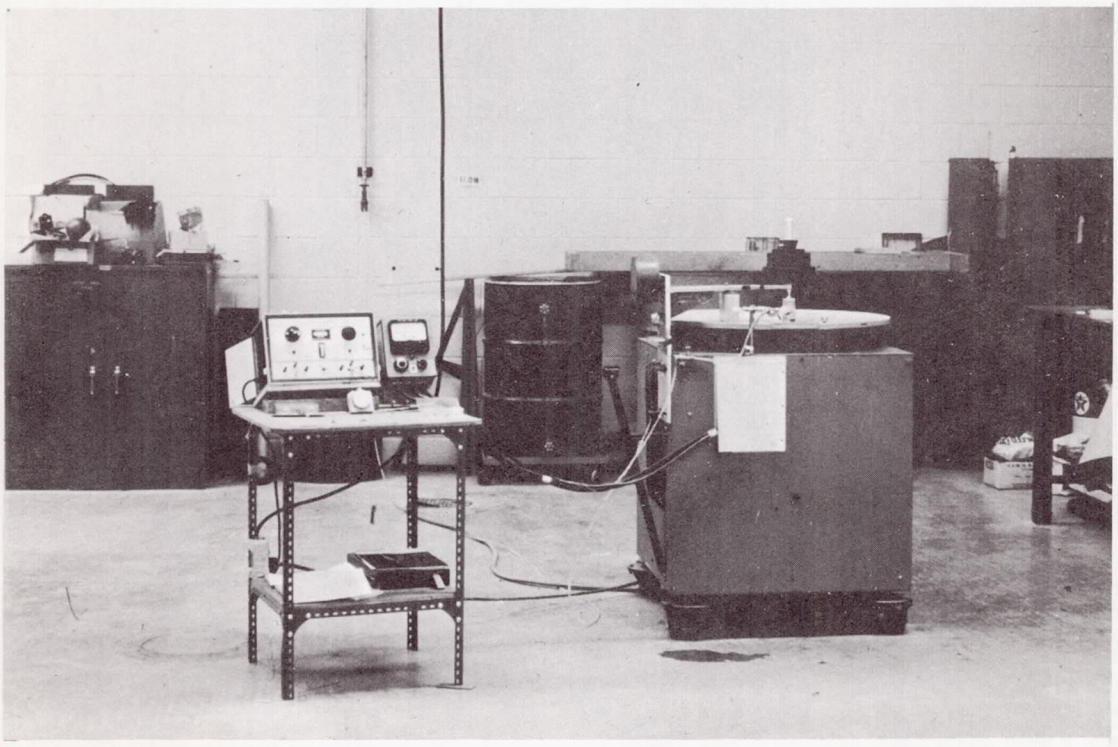

Figure 3. Photograph of test apparatus.

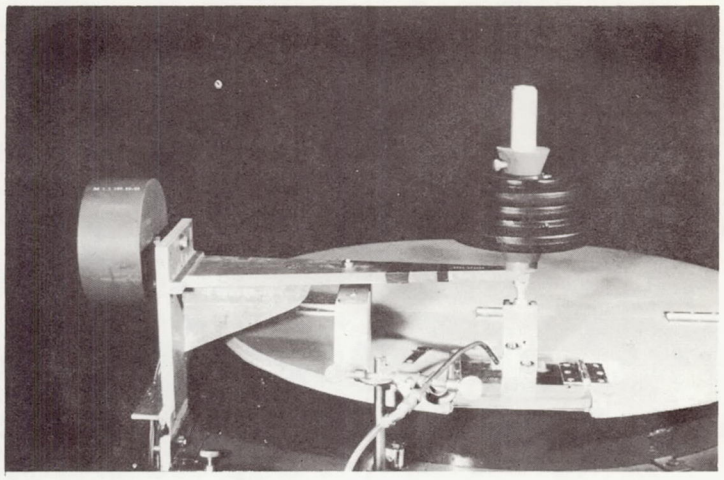

Figure 4. Photograph of test apparatus.

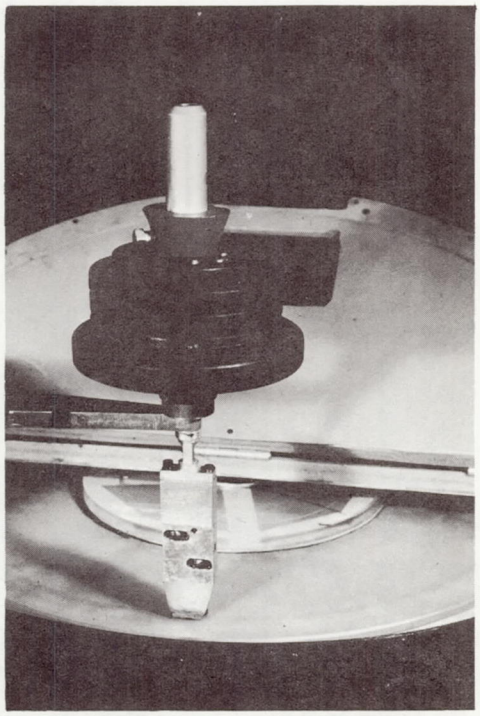

Figure 5. Photograph of test apparatus.

Friction Testing Machine - Front View

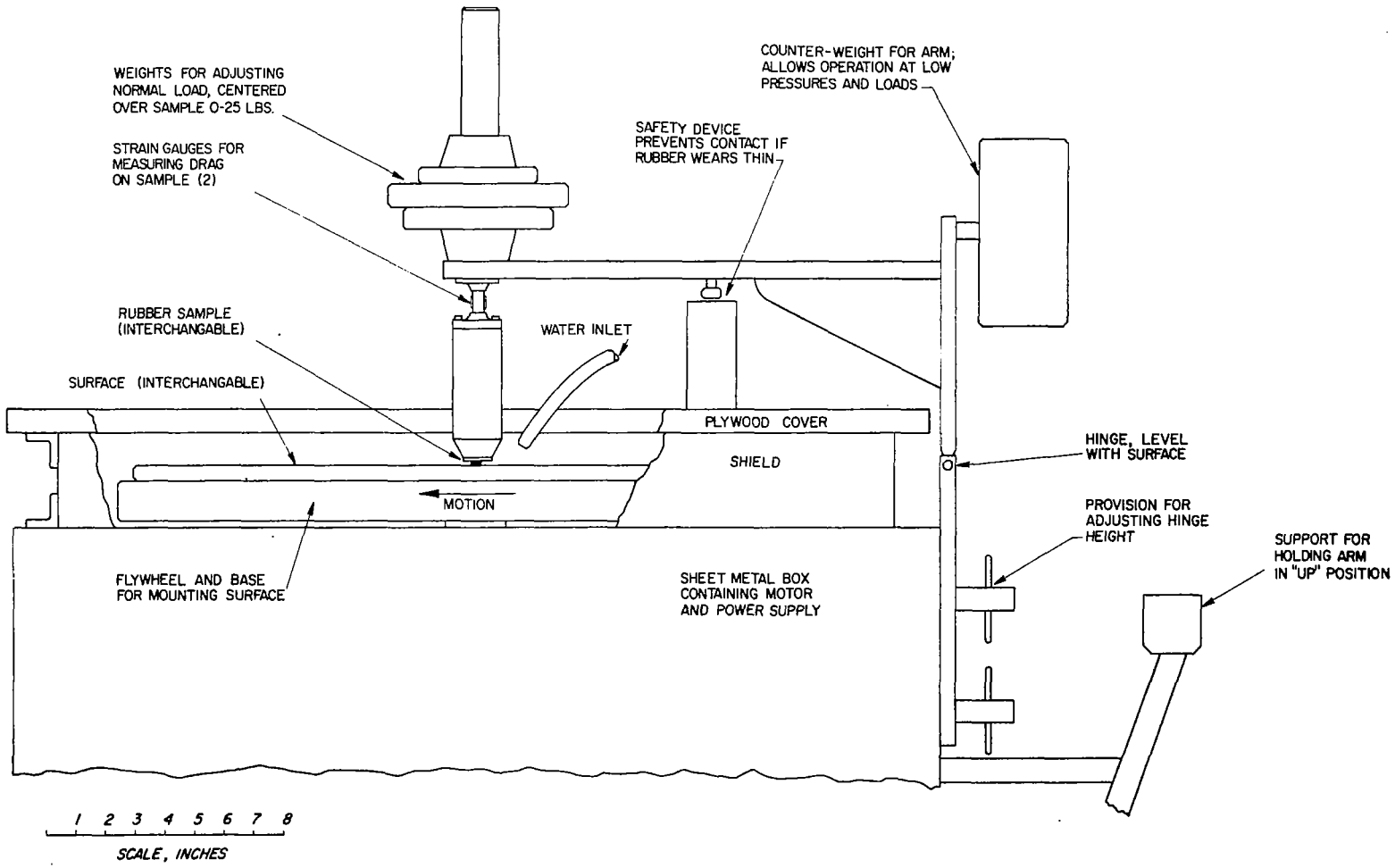

Figure 6. Drawing of test apparatus.

the end of the arm can be varied to effect a normal contact pressure variation of from 8 to 400 psi, based on total force applied and using a 1/4 $in.^2$ area of contact. The hinge in Figure 6 allows the arm to be raised for access to the rubber sample, while the limit stop under the arm is a safety device to prevent contact between the steel mount and the test surface.

The electric motor driving the rotating turntable has a tachometer feedback system for accurate speed control, independent of torque. This system has a usable speed range of 90 to 1500 rpm, which corresponds to 5.3 mph to 89.3 mph on a 10-in. radius. Interchangeable test discs rest, like records, on the balanced aluminum turntable. The test discs used during these tests were smooth aluminum and rough and smooth glass. The 2024T4 aluminum disc was originally anodized, although this coating had worn off by the end of the testing. The roughness was 2-5 μin. rms in the direction of travel, and 30-40 μin. rms across the direction of travel. The plate glass disc used as a friction surface was polished on one side and sand-blasted on the other. The polished surface had a roughness of 0.25 μin. rms. Under a microscope the surface appeared as a very smooth surface with slight pock marks. The sand-blasted disc had a roughness of 150-200 μin. rms, with random, very ragged asperities.

A lubricant, usually water, was fed through a tube to an outlet directly in front of the test sample. Preliminary tests with lubricant flow rate showed no dependence of friction on flow rate within the range of the apparatus, as long as the flow rate was great enough to insure a thin lubricant film in front of the sample. This may have been due to the fact that the rotating disc tended to throw excess lubricant. Because of the wide range of acceptable flow rates,

an arbitrary moderate flow rate of approximately 1/16 gal/min was used during all tests.

C. TEST SAMPLES

The rubber test blocks used in these experiments were prepared in several ways, depending on their geometry. The square rubber blocks were cut with a knife from the various larger specimens into 1/4 in. x 1/4 in. squares, approximately 3/32 in. thick. These squares were then mounted on 1 in. x 1/2 in. x 1/8 in. steel plates with Eastman 910 contact cement. The samples were frozen with liquid nitrogen and the test surface milled to achieve a fairly flat, uniformly textured surface.

The round samples were prepared in a slightly different way. A 3/32 in. thick rubber sheet was cut from the molded rubber blocks and sanded on the cut side until a fairly flat and smooth surface was achieved. Cylindrical rubber blocks were cut from this sheet with a 9/32 in. diameter cork cutter and mounted on the steel plates, sanded side down, with Eastman 910 cement. Thus the test surface of the round samples was the original surface of the molded rubber block, while the test surface of the square samples was a freshly milled surface. To check any differences that might result from these two methods of preparation, a round sample was tested, then frozen and milled and retested. The frozen and milled surface had a 13% higher drag value than the original surface. Our conclusions, however, are based only on comparisons of samples of similar geometry and construction, in order to eliminate any differences due to sample preparation and geometry.

Eight types of rubber were used in these tests, with pure natural and

synthetic rubbers given the most extensive testing. Table I lists the rubbers, the source of the samples and their approximate composition where it is known.

TABLE I

LIST OF RUBBER COMPOSITIONS TESTED

Rubber Type	Approximate Composition	Source
B107-1T	100% natural rubber	Uniroyal sample block
B108-1T	100% natural rubber with additives to improve heat aging characteristics and reduce stock reversion	Uniroyal sample block
B109-1T	100% synthetic rubber (polybutadiene)	Uniroyal sample block
B110-1T	100% natural rubber with additives to reduce heat degradations and with modification to curing cycle	Uniroyal sample block
B111-1T	Blend of natural rubber and polybutadiene	Uniroyal sample block
Aircraft	Unknown	Aircraft tire tread
Pirelli	Unknown	Automobile tire tread (Pirelli)
Michelin	Unknown	Automobile tire tread (Michelin)

D. TEST PROCEDURE

The prepared samples were mounted on the sample holder and lowered onto the test disc. Each sample was "zeroed" by eliminating the normal load bending moment with the fore-aft adjustment. The sample was lifted off the disc, a zero was recorded and the disc was accelerated to testing speed. Lubricant flow and normal load were adjusted to desired test conditions. The untreated samples were lowered gently onto the disc. Drag readings were taken at 1/12,

1/2, 1, 5, and 10 min after touchdown. The sample was then lifted off the disc and a zero recorded to check zero drift. The arm was raised for sample treatment as shown in Figure 7. For temperature treatment the aluminum block was checked for correct temperature with the pyrometer and then pressed against the rubber test surface for 2-10 sec with approximately 20 psi pressure. The sample was allowed to cool for 5-10 sec while the arm was lowered and the zero recorded with the sample free of the disc. The treated sample was then lowered

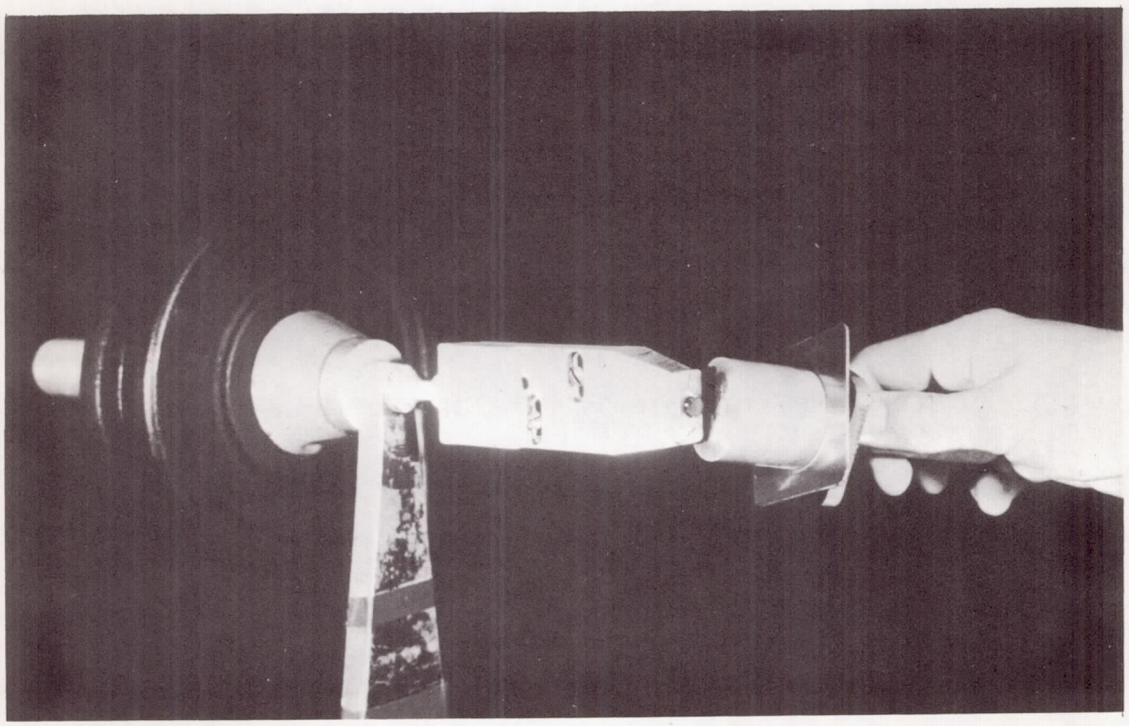

Figure 7. Photograph of sample being surface treated with a hot block

onto the disc and drag readings again taken at 1/12, 1/2, 1, 5, and 10 min after touchdown. Any further treatment was done in a similar manner. Pressure and velocity tests were run with the sample in place by varying the normal load or disc velocity over the test range. At this point it should be emphasized that all of the testing discussed in this report was done on a lubricated surface, and that no dry friction tests were attempted.

E. EXPERIMENTAL RESULTS

Five types of tests were run with temperature-treated and untreated rubber. Applied treatment temperature, average contact pressure, disc velocity, lubricant viscosity and rubber sample geometry were the primary variables.

Standard values of 203 psi, 17.9 mph sliding speed on 10-in. radius, and water lubrication were used when varying applied surface temperature. Figures 8-14 show the effect of applied temperature treatment on friction drag for eight kinds of square rubber samples on a smooth aluminum surface. Figure 15 shows the same friction drop at high treatment temperatures for round natural rubber samples on smooth aluminum and smooth glass. Figures 16 and 17 show the effect of treatment temperature on friction drag for round natural and synthetic rubber samples on rough glass. Note that both high and low values were obtained in the later tests, depending on how the aluminum treatment block was pressed against the sample surface. Pressing the treatment block straight-on, with no rotation or sliding of the block on the rubber, resulted in the higher values of friction. Pressing the treatment block against the leading edge of the sample, or pressing the block against the whole surface with a tilting, rotation

or sliding motion resulted in a low set of friction values. This strongly suggests that some form of slider bearing action is operative here, where the presence of a chamfered or tapered lip is necessary to allow the water film to form under the leading edge of the sample. When no such tapered lip is present, the leading edge may tend to wipe the surface dry causing a much higher friction value.

In neither case was a visible deposit of rubber left on the test disc after friction testing.

In searching for a means of eliminating the low friction of reverted rubber, slitting, siping and other surface geometry changes were investigated. Figure 18 shows the effect of increasing numbers of slits on the friction of round natural rubber samples treated at 600°F. The slitting effects are shown for both smooth and rough glass surfaces. In addition, various specimen geometries were run on smooth glass in an attempt to determine the effect of the length and shape of the leading edge on the friction of treated rubber. However, no marked effects of specimen geometry were observed.

Untreated natural rubber samples running on smooth glass show some variation in friction characteristics. Reproducibility is not too good. Tests to determine the effect of sanding and scraping the samples were run on smooth glass. These are primarily tests of surface cleanliness and roughness. The results of two of these tests are shown in Figures 19 and 20.

The effect of contact pressure on friction drag for untreated and treated natural rubber is shown in Figure 21. The effect of the three test surfaces on these curves is also shown there.

The same type of tests were run with velocity as the controlled variable. Figure 22 shows friction variation with speed for square natural rubber samples on smooth aluminum. Figures 23 and 24 show the added effect of lubricant viscosity on the velocity-friction curves. Friction variation with velocity is shown for two lubricants with round natural rubber samples on smooth and rough glass. Figure 25 shows how the general velocity-friction curve changes shape with differences in normal pressure. This test was run on rough glass with treated natural rubber samples.

Conventional friction tests were run with varying lubricant viscosity. The results are shown in Figures 26 and 27. The natural rubber samples were run on smooth and rough glass with standard pressure of 201 psi and standard velocity of 17.9 mph.

Because a characteristic of reverted rubber is the hydrophobic nature of the surface, different lubricant tests were run on smooth aluminum to determine if surface tension had any effect on treated rubber friction. Contact angle measurements were taken for each treatment temperature applied to the rubber specimen and correlated with friction values obtained for the same treatment temperature. Because of the difficulty in getting accurate measurements of contact angle, no consistent correlation between contact angle and friction could be found. Reducing surface tension of the lubricant had no apparent effect on the friction of either treated or untreated rubber. Kodak Photo-flo, Cascade dishwasher detergent and Tide detergent solutions were used to significantly lower the surface tension of the water lubricant with no significant effect on friction drag.

From the nature of the experimental data which has been presented, it may be seen that by far the most important single conclusion which may be drawn is that surface temperatures of 450° to 600°F applied to a natural rubber sample will greatly reduce its subsequent friction coefficient on a smooth wet surface. Other factors may modify the numerical friction values, but the basic influence of the rubber which has been heat-reverted remains. Evidence seems to be that some sort of liquid film bearing is operative here, since the low friction values of reverted rubber occur at room temperature in the absence of heat or steam, seem to be most prevalent when geometric conditions favor formation of a water wedge under the leading edge, and agree in magnitude with hydrodynamic bearing theory.

Finally, the average friction coefficients and average deviations taken from the test data are summarized in Table II.

TABLE II

DRAG AVERAGES AND DEVIATIONS FOR FRICTION SPECIMENS

	Rubber:	B107-1T	B108-1T	B109-1T	B111-1T	B107-1T	B107-1T	B107-1T		B109-1T
	Geometry:	square	square	square	square	round	round	round		round
	Surface:	aluminum	aluminum	aluminum	aluminum	aluminum	smooth glass	rough glass		rough glass
Untreated	Initial f_o (avg)	.129	.109	.097	.053	.034	.072	.240		.210
	Avg deviation	.008	.009	.011	.007	.008	.016	.010		.002
		6%	8%	11%	13%	23%	23%	4%		1%
	10 min f'_o (avg)	.100	.082	.064	.029	.023	.051	.224		.196
	Avg deviation	.011	.007	.012	.006	.005	.010	.008		.003
		11%	9%	19%	20%	21%	20%	3%		1%
	No. of samples tested	17	15	15	16	5	7	15		3
Treated at 600°F								high value	low value	low value
	Initial f (avg)	.011	.008	.033	.010	.016	.024	.222	.102	.109
	Avg deviation	.005			.001	.007	.004	.009	.009	
		45%			10%	46%	17%	4%	9%	
	10 min f' (avg)	.010	.007	.011	.009	.010	.019	.201	.097	.094
	Avg deviation	.004			.002	.003	.003	.009	.009	
		39%			18%	28%	17%	5%	10%	
	No. of samples tested	2	1	1	2	5	7	3	5	1

f = friction coefficient.

V. HYDRODYNAMIC BEARING THEORY ANALYSIS

Hydrodynamic bearing theory can be used to predict the forces associated with pure viscous drag. (Ref. 3). Assumptions of laminar flow of a Newtonian fluid between a flat smooth surface and a flat smooth bearing at a moderate angle of attack are used in this analysis.

The total drag on the bearing is given by

$$F_R = \frac{1}{\sqrt{6}} bk_{fr} \left(\frac{\mu \ell V P_{av}}{k_p \eta} \right)^{1/2}$$

where b = width of bearing

ℓ = length of bearing

P_{av} = average pressure

V = velocity of sliding

μ = absolute viscosity of lubricating film

F_r = total viscous and pressure drag

K_p = dimensionless factor determined by the geometry of the contact area

η = dimensionless factor to correct for fluid outflow from the sides of the bearing

K_{fr} = dimensionless factor determined by the geometry of the contact patch

The factors K_p and K_{fr} are abbreviations for formulas which are derived analytically but which require considerable calculation. The factor η is a semi-empirical correction used to correlate three dimensional bearings with two dimensional theory.

Some of the geometry must be assumed. Referring to Figure 28 we may define $m' = \frac{h_1}{h_0} - 1$. This quantity must be assumed in order to determine K_p and K_{fr}.

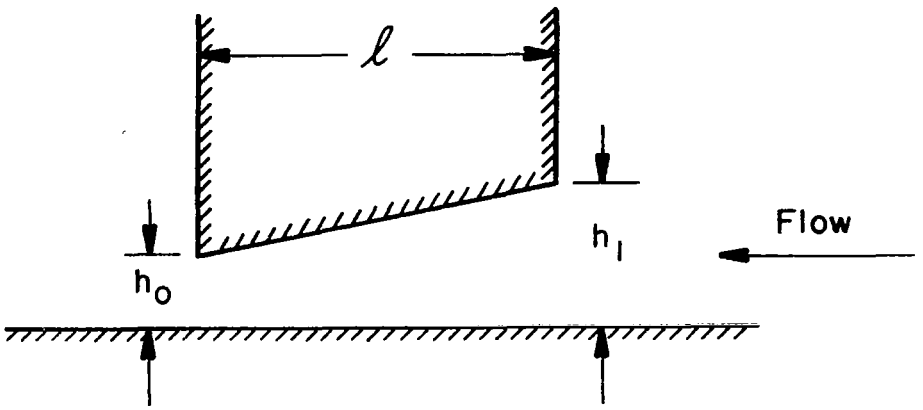

Figure 28. Slider bearing geometry.

The water film thickness is h_1 at the entrance or leading edge and h_0 at the trailing edge. The values m' = 1, $h_1 = 2h_0$ are taken by Fuller to be a representative value and is used in many of the calculations which follow.

The film thickness may be found using the expression

$$h_0 = \left(\frac{6\mu V \ell \eta K_p}{P_{av}} \right)^{1/2}$$

Some representative values are

$$b = \ell = 1/4" = 1/48' \quad b/\ell = 1; \ \eta = 0.440$$

$$\mu = 2 \times 10^{-5} \text{ lbsec/ft}^2$$

$$V = 26.2 \text{ ft/sec}$$

$$P_{av} = 202 \text{ lb/in.}^2$$

$$m' = 1$$

We then have

$$h_o = 5.15 \times 10^{-6} \text{ ft} = 61.8 \times 10^{-6} \text{ in.}$$

This yields an angle of attack of approximately

$$\frac{h_1 - h_o}{\ell} = .00024 \text{ radians}$$

By treating one of the parameters as variable and holding others fixed at the representative values, we arrive at the relations

$$F_R = 24.2 \times 10^{-4} \overline{P_{av}} \quad (F = \text{lb}, P_{av} = \text{psi})$$

$$F_r = .00668V \quad (F = \text{lb}, V = \text{ft/sec})$$

These relations give the theoretical curves for drag of square bearings as shown in Figures 21, 22, 24, 26, and 27.

Although the geometric factors may change when hydrodynamic bearing theory is applied to round bearings, the dependence of drag on viscosity, velocity, and normal pressure should be the same. Thus, the curves may be shifted in magnitude, but the general shapes should remain the same as those for square bearings.

VI. CONCLUSIONS

One of the problems with friction measurements is reproducibility. In the present tests reproducibility was quite good. Table II gives the friction data, with averages and standard deviations, for untreated rubber and rubber treated at 600°F. The problem of friction scatter of untreated rubber on smooth glass can be attributed to slight geometry differences in the leading edge of various samples. This becomes important when the asperity height is reduced to a very small value, as on smooth glass. Figures 19 and 20 show how slight sanding of the rubber sample changed its friction coefficient. The friction drag values exhibited much less scatter after sanding, as mentioned in Ref. 4. From the rough glass tests, it was found that the slight sanding caused the data to fall closer together than simply running the samples as cut, as evidenced by the small deviation values in Table II. The problem did not arise when using the aluminum disc because the square samples tested on the aluminum were all frozen and milled to give a more uniform surface. In addition, the aluminum disc was at least 10 times rougher than the smooth glass, where samples must be sanded in order to get any kind of reproducibility.

In successive tests of the same sample, drag values agreed to within 3-5%. The original test was run, either treated or untreated, followed by a time delay of 16-48 hours and a retesting under the same conditions as the original. The resulting small scatter of friction values reflected the precision of the apparatus and showed that most of the friction scatter was due to slight variation in individual sample geometry and surface conditions.

From Figures 8 through 14 it is apparent that any treatment temperature above a critical value has a large effect on friction. All eight rubber compositions tested have a drop in friction when subjected to temperature treatments above the 450°F-500°F range. The square samples on the aluminum disc as shown in Figures 8 through 14, show a minimum friction after a 550°F-600°F temperature treatment. Figure 15 shows that this drastic friction drop also occurs with round samples on aluminum and smooth glass.

The round samples on rough glass gave two different sets of friction readings, as shown in Figures 16 and 17, depending on how the treatment block was pressed against the rubber. The straight-on, uniform pressure treatment gave high friction values, close to those given by the untreated samples. These high friction values can be explained by the condition of the leading edge, since microscopic inspection of the samples after testing revealed that the leading edge had worn off at approximately a 45° angle.

Treatment at uniform pressure leaves only the flat test surface of the sample exposed to the treatment block. Because the 200 psi normal pressure and 17.9 mph speed on rough glass gives a large drag force, distortion of the sample during the run is great enough to bring the untreated leading edge into contact with the glass. This untreated edge, which is stronger and harder than the soft, pliable treated patch, is an effective wiper. This wiping action of the leading edge effectively reduces the film thickness of the lubricant under the whole contact patch. If the treatment block is moved and tilted during treatment, the leading edge is exposed to the high temperature block. Distortion during testing only results in more treated rubber acting as the leading edge.

This soft, pliable leading edge is not as effective a wiper as the untreated rubber, and a thicker lubricant film might be present in the contact patch.

The two values of friction coefficient are not observed on smooth glass because of the much smaller asperity height. Any temperature treatment, whether or not it affects the leading edge, would expose enough of this leading edge to the high temperature to assure a soft pliable edge during testing. The smaller asperity height and subsequent lower drag would not cause extensive distortion during testing. Thus much less of the leading edge would come into contact with the smaller asperities during this distortion. The smaller asperities also require a thinner layer of soft, pliable treated rubber to provide the low local contact pressures over the asperity tips. A greater lubricant film thickness may thus be maintained. Such a line of reasoning has previously been advanced by both Saal[5] and Grosch and Maycock[6].

The effect of temperature treatment on pressure-friction curves is seen in Figure 21 for the three disc surfaces. The low friction coefficients for the aluminum disc seem to approach hydrodynamic bearing theory much better than the curves for the glass surfaces. Because the smooth glass is the flatest and smoothest, one might expect its friction curves to best approach bearing theory. One explanation for the low friction values of the aluminum disc is based on the very slight groove worn in the aluminum due to repeated testing. The groove is less than 0.005 in. deep, and is smoothest in the direction of travel, indicating that polishing occurred. Since this groove is deeper than the liquid film thickness under the sample predicted by bearing theory, the groove could reduce lubricant flow out the sides of the contact patch. This could modify

the geometry of flow and cause a more effective bearing to exist than predicted by simple conventional bearing theory.

The velocity vs. drag curves of Figures 22 through 25 show the effect of normal pressure, viscosity and disc surface on sample friction. At low velocity, high pressure and with water as a lubricant the experimental curve is much higher than the predictions of bearing theory. As the predicted film under the contact patch gets thicker, due to lower pressure or higher viscosity, the experimental and calculated friction curves come closer together.

The limitations on the velocities which can be obtained are mainly associated with disc speed, since stresses in the glass or aluminum friction plates limit the available sliding speeds. In addition, only a limited variation in lubricant viscosity is attainable with mixtures of glycerine and water as used here.

Figures 26 and 27 show that higher viscosity lubricants on smooth glass increase drag, while on rough glass they decrease drag. This difference can be explained in terms of the large difference in the asperity height of the two surfaces. On smooth glass, which approaches the bearing theory approximation of a flat smooth surface, the drag would be mostly the viscous drag of the liquid film. The more viscous lubricants between bearing and surface would have greater drag. On rough glass, whose asperities cannot be taken into account in bearing theory, the more viscous fluid would tend to hide the asperities, and to eliminate the mechanical interaction between the asperity tips and the rubber surface (Refs. 5, 6, 7). Then the higher the viscosity of the lubricant, the lower the drag until such time as the viscous drag is greater

than the mechanical drag and the total drag starts increasing.

If one qualitatively incorporates the mechanical and geometric properties of both solid surfaces into a viscous drag bearing theory, one can give an explanation for the low friction of reverted rubber. Saal[5] originally worked in this area in 1935 with apparatus very similar to the one used in these experiments. Saal assumed a hard smooth rubber surface and qualitatively included lubricant and pavement properties. Gough and Badger[7] mention rubber tread patterns, but neglect the rubber mechanical properties. Experimentally, the effect of both surfaces is shown on the pressure, velocity and viscosity vs. drag curves of Figures 21 through 27. The effect of the pavement surface is shown by the different curves for the three disc surfaces, while the effect of the rubber surface is shown in the different results for untreated and treated rubber. As Saal pointed out, if both surfaces are flat and perfectly smooth bearing theory predicts only viscous drag. If the pavement surface has asperities which provide high local contact pressures at their tips, then some kind of direct mechanical friction is involved. Bevilacqua and Percarpio[4] call this mechanical friction abrasion. The mechanical friction on a rough surface is much larger than viscous drag, especially if the rubber surface is hard and not easily deformed. However, if the rubber surface is soft and pliable, then the rubber can deform easily around the asperities, lower the localized contact pressure and eliminate some of the direct mechanical friction. If the asperities are small enough, the reverted rubber deep enough or the lubricant viscous enough, then viscous drag prevails. Thus, for a given disc surface, soft pliable treated rubber promotes low viscous hydroplaning friction whereas hard

untreated rubber promotes some kind of mechanical friction which dominates the viscous drag.

Because the reverted rubber was tested at room temperature with cool water, and because the differences between normal and reverted rubber friction exist down to low speeds and pressures, it is believed that the low observed friction is not due to steam formed in the contact patch. Not having enough experience in "reversion" accidents to argue against the presence of steam during the skids, it can only be noted that the extremely low friction values of reverted rubber found in the laboratory experiments existed without steam. Thus, it is believed steam may be a result of the skids but is not the cause of low friction of "reverted" rubber.

Since the water on airport runways can only be controlled within rough limits, any solution to the reversion problem probably lies in the controlling the two surfaces. However, viscous mixtures of water, dust and oil deposits which may appear on a runway during the initial minutes of a light rainfall following a prolonged dry period may increase the probability of viscous hydroplaning. Occasional cleaning of runways in dry areas may prevent this formation of viscous lubricant mixtures. The rubber surface can be controlled in two possible ways—compounding of the tread rubber and changing tread geometry with sipes and grooves. Since all eight types of rubber tested exhibited low friction in the reverted state, rubber compounding seems to offer slight chance of preventing the low friction of "reverted" rubber. Siping and grooving, although possibly giving a friction increase over the smooth rubber surface, might be too costly in terms of tire wear or tread chunking problems.

Control of the runway surface is probably the best way to eliminate the low friction of "reverted" rubber. Unpolished clean runways can supply asperities large enough and sharp enough to cancel the effect of the soft, pliable rubber surface. Runway gooving, recently tested by NASA and now in limited test use for preventing hydroplaning, could reduce or eliminate the low friction of "reverted" rubber on aircraft tires. The groove edges could provide the large local contact pressures needed to break through a liquid film to the "reverted" rubber, and to restore normal friction forces.

VII. REFERENCES

1. Obertop, D.H.F., "Decrease of Skid-Resisting Properties of Wet Road Surfaces at High Speeds," ASTM Special Technical Publication No. 326, June 1962.

2. Horne, Walter B., Yager, Thomas J. and Taylor, Glenn R., "Recent Research on Ways to Improve Tire Traction on Water, Slush or Ice," AIAA Aircraft Design and Technology Meeting, November, 1965.

3. Fuller, Dudley D., "Lubrication Mechanics," Section 22 of "Handbook of Fluid Dynamics," Victor L. Streeter, editor-in-chief, McGraw-Hill, New York, 1961.

4. Bevilacqua, E.M. and Percarpio, E.P., "Friction of Rubber on Wet Surfaces," Science, 160, May 31, 1968.

5. Saal, Dr. R.N.J., "Laboratory Investigations into the Slipperness of Roads," Chemistry and Industry, January 3, 1936.

6. Grosch, K.A. and Maycock, G., "Influence of Test Conditions on the Wet Skid Resistance of Tire Tread Compounds," RAPRA Code No. 6T103-9521, Transactions, 42 December 1966.

7. Gough, V.E. and Badger, D.W., "Tires and Road Safety," Fifth World Meeting of the International Road Federation, London, September 1966.

EXPLANATION FOR FIGURES 8-17

Friction Coefficient f vs. Treatment Temperature

Samples 1/4 in. x 1/4 in. square, 9/32 in. dia. round

Load: 12.7 lb.

Mean Contact Patch Pressure: 203 psi

Velocity: 17.9 mph = 26.2 ft/sec

Lubricant: Water

Surfaces: Aluminum—aluminum oxide, rough and smooth glass

Ambient Temperature: 75-80°F

Legend: △▽ Reading taken 0-5 sec after touchdown.

□◇ Reading taken 10 min after touchdown.
This closely approximates an equilibrium friction coefficient value.

Untreated room temperature data points represent an average of several trials.

This data is shown at the 80°F position.

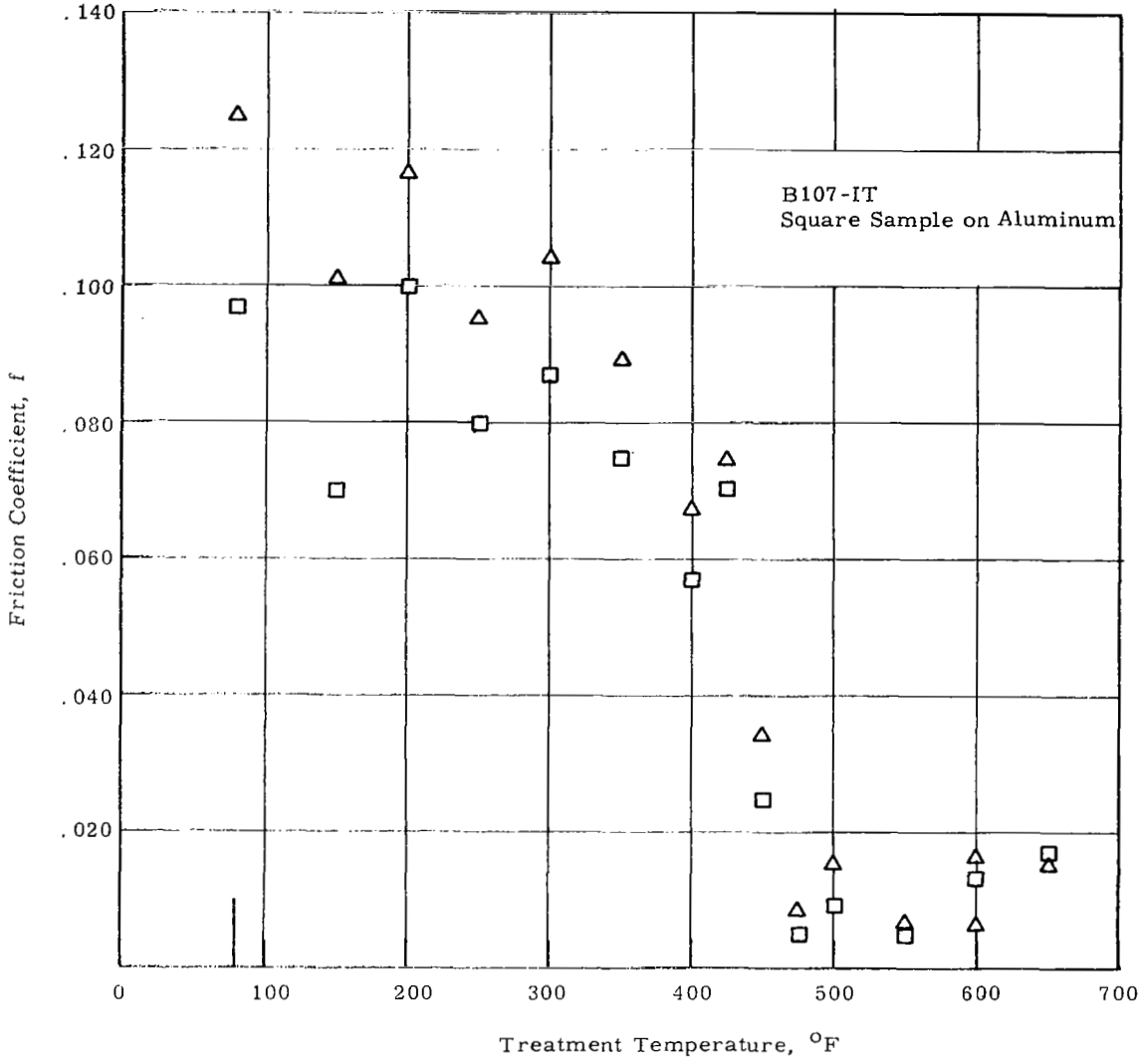

Figure 8. Friction coefficient vs. treatment. Temperature for Sample B107-1T.

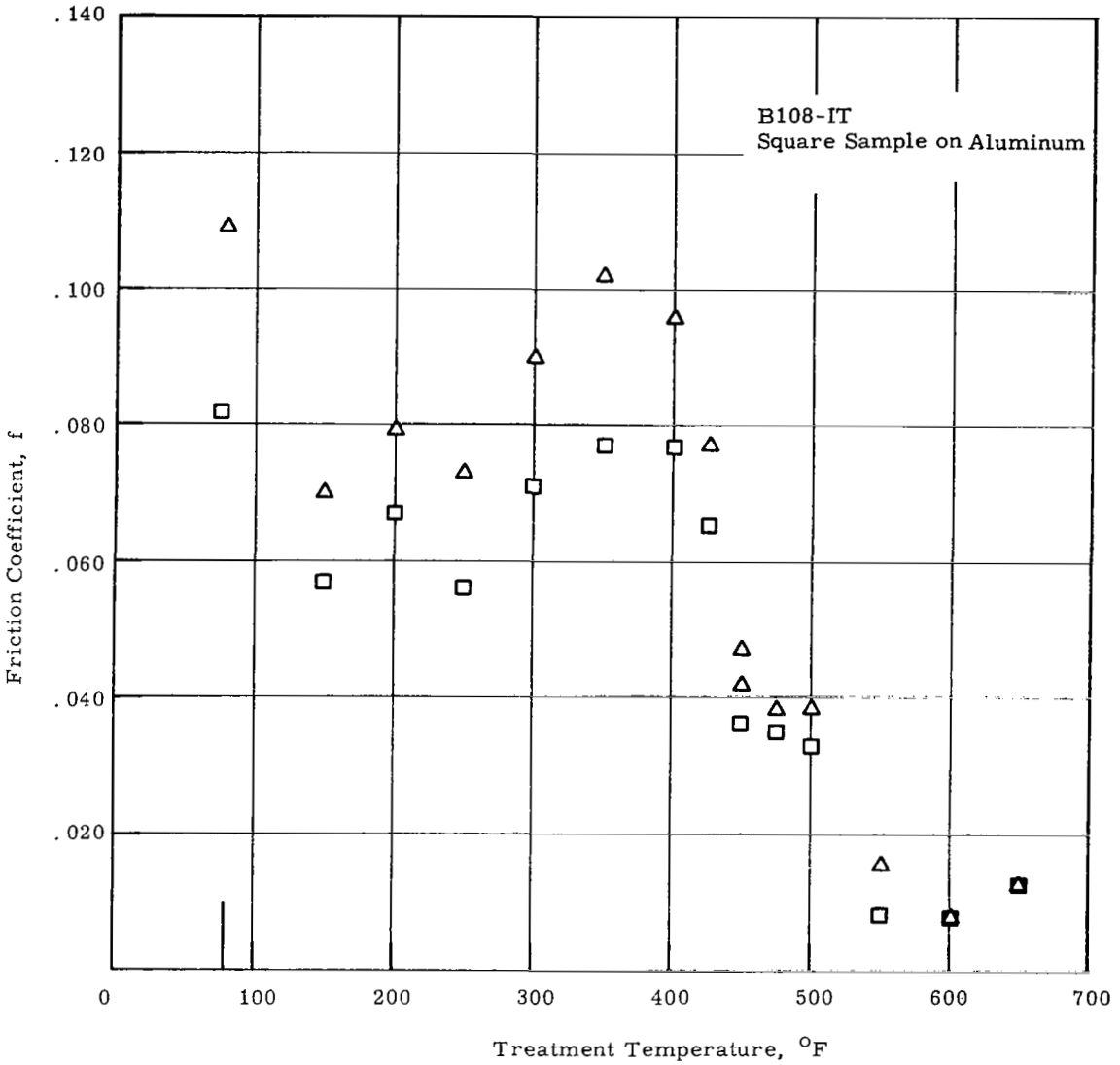

Figure 9. Temperature for Sample B108 1T.

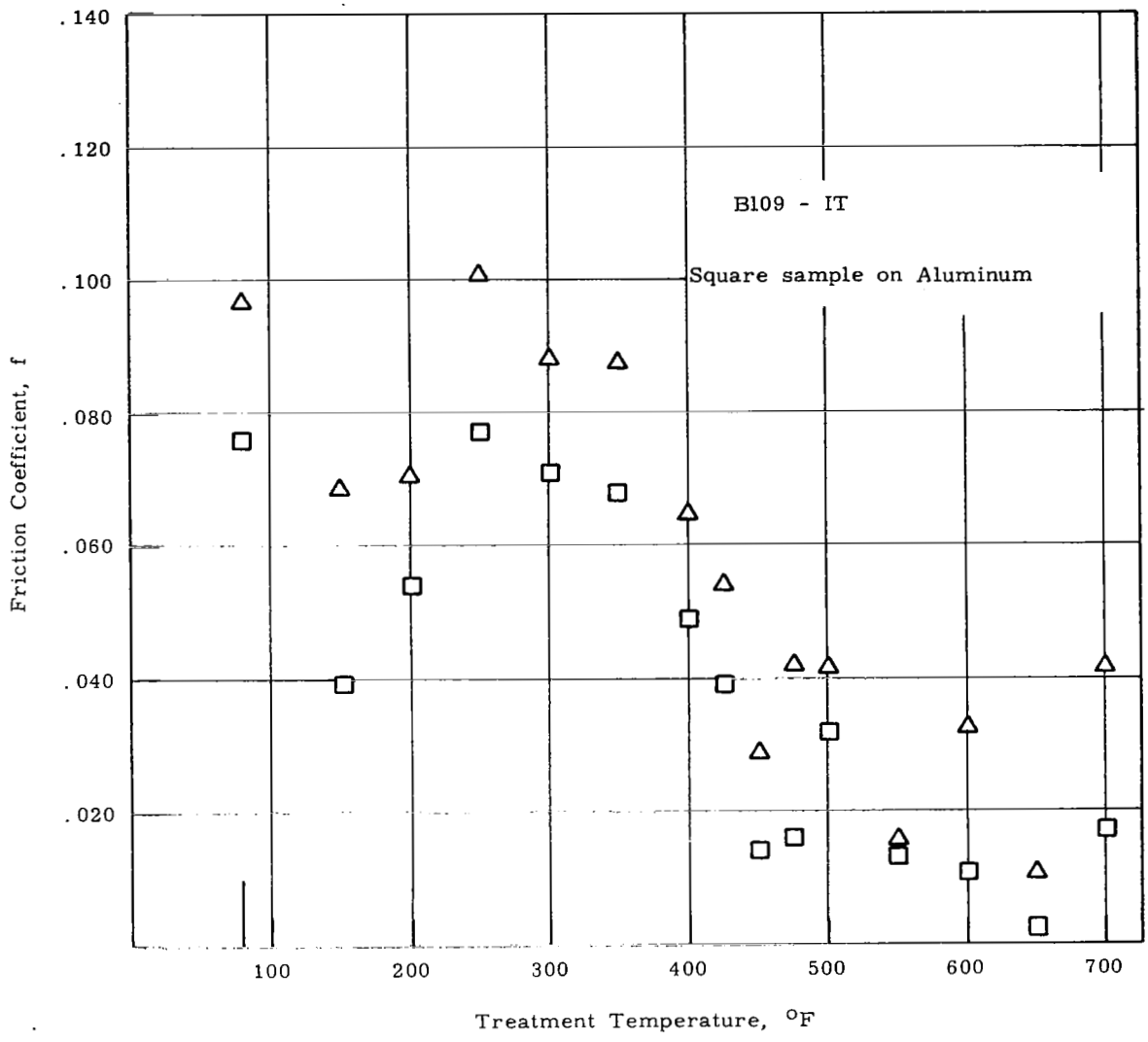

Figure 10. Temperature for sample B109-1T.

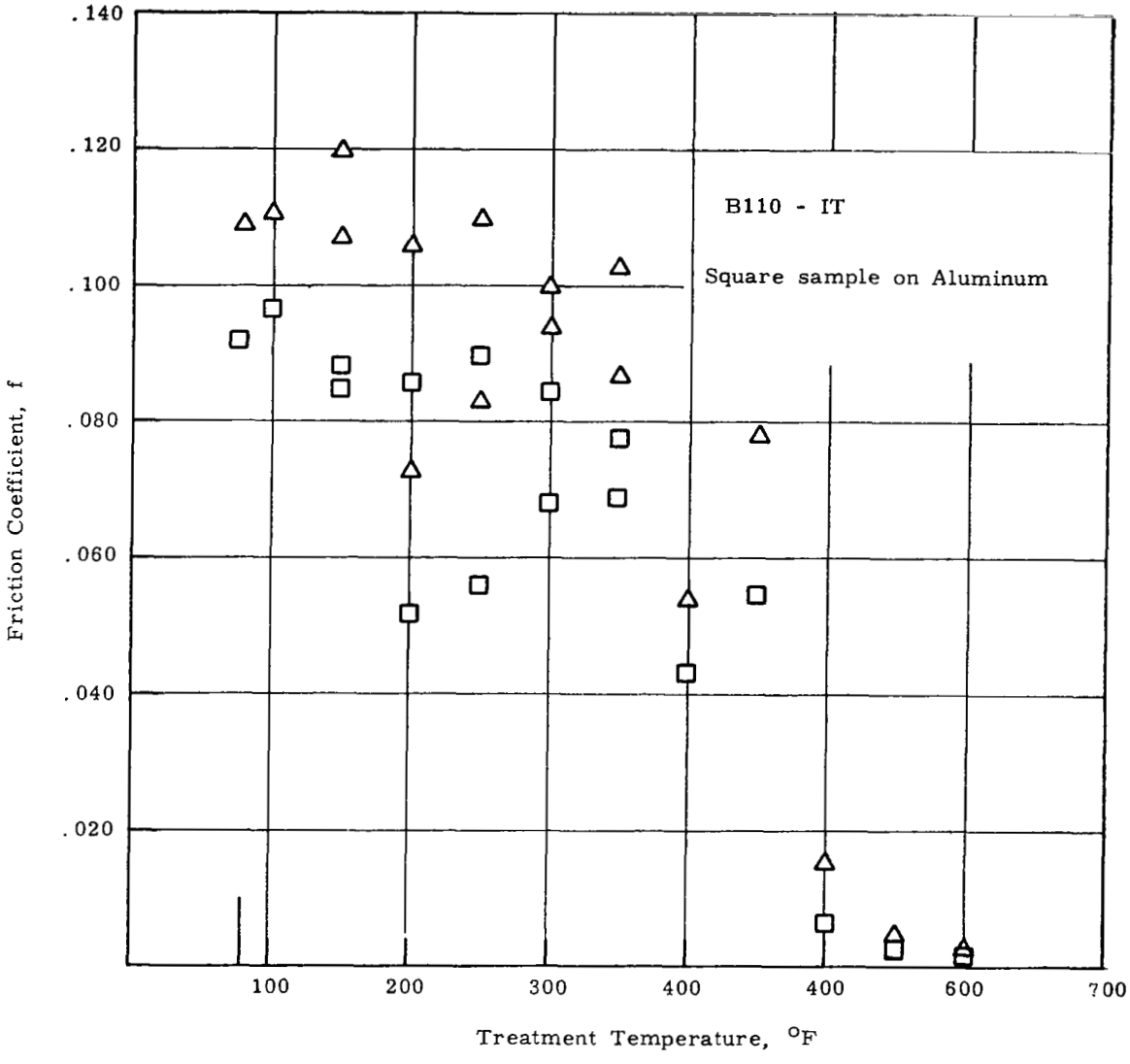

Figure 11. Temperature for sample B110-1T.

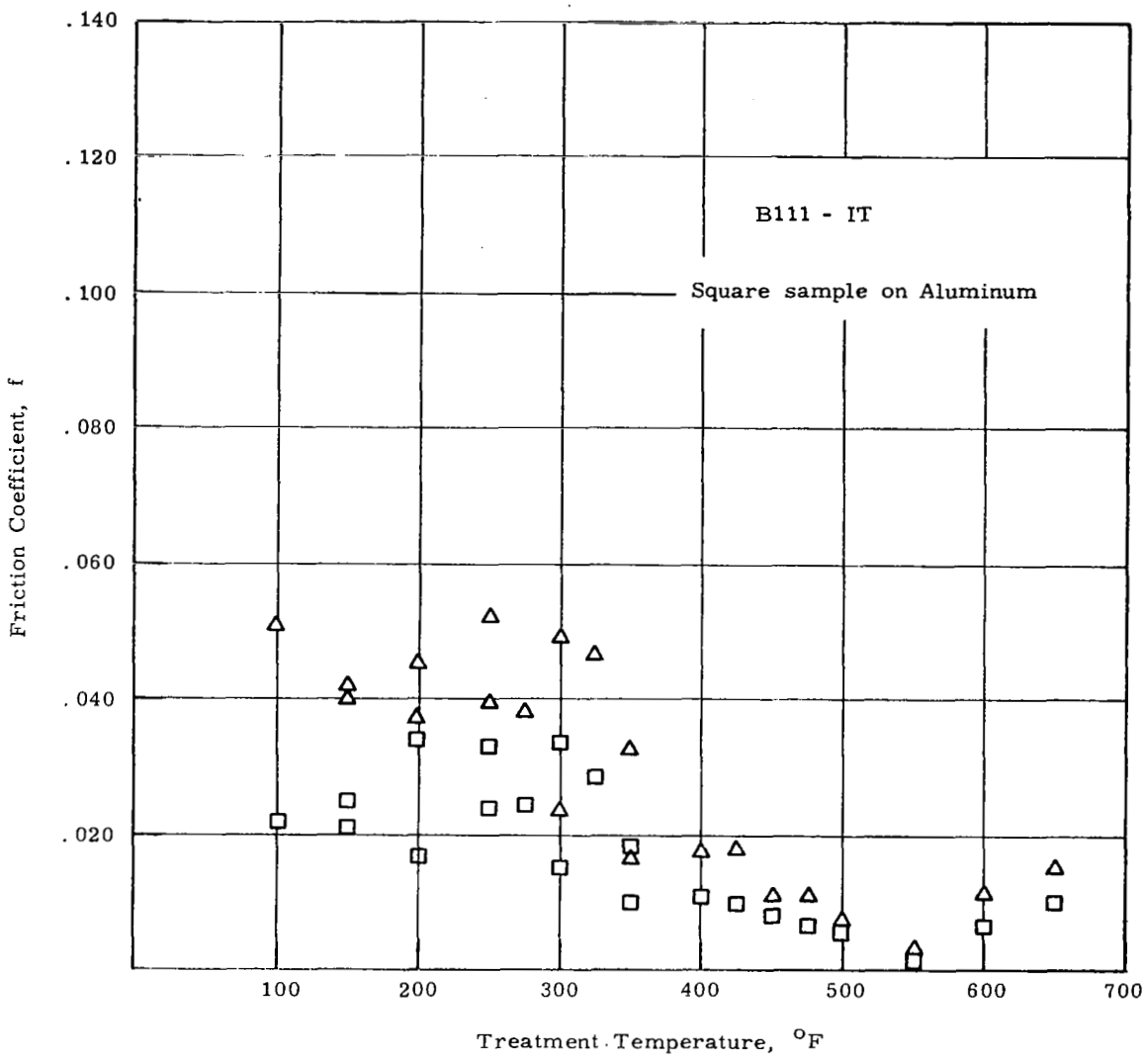

Figure 12. Temperature for sample B111-1T.

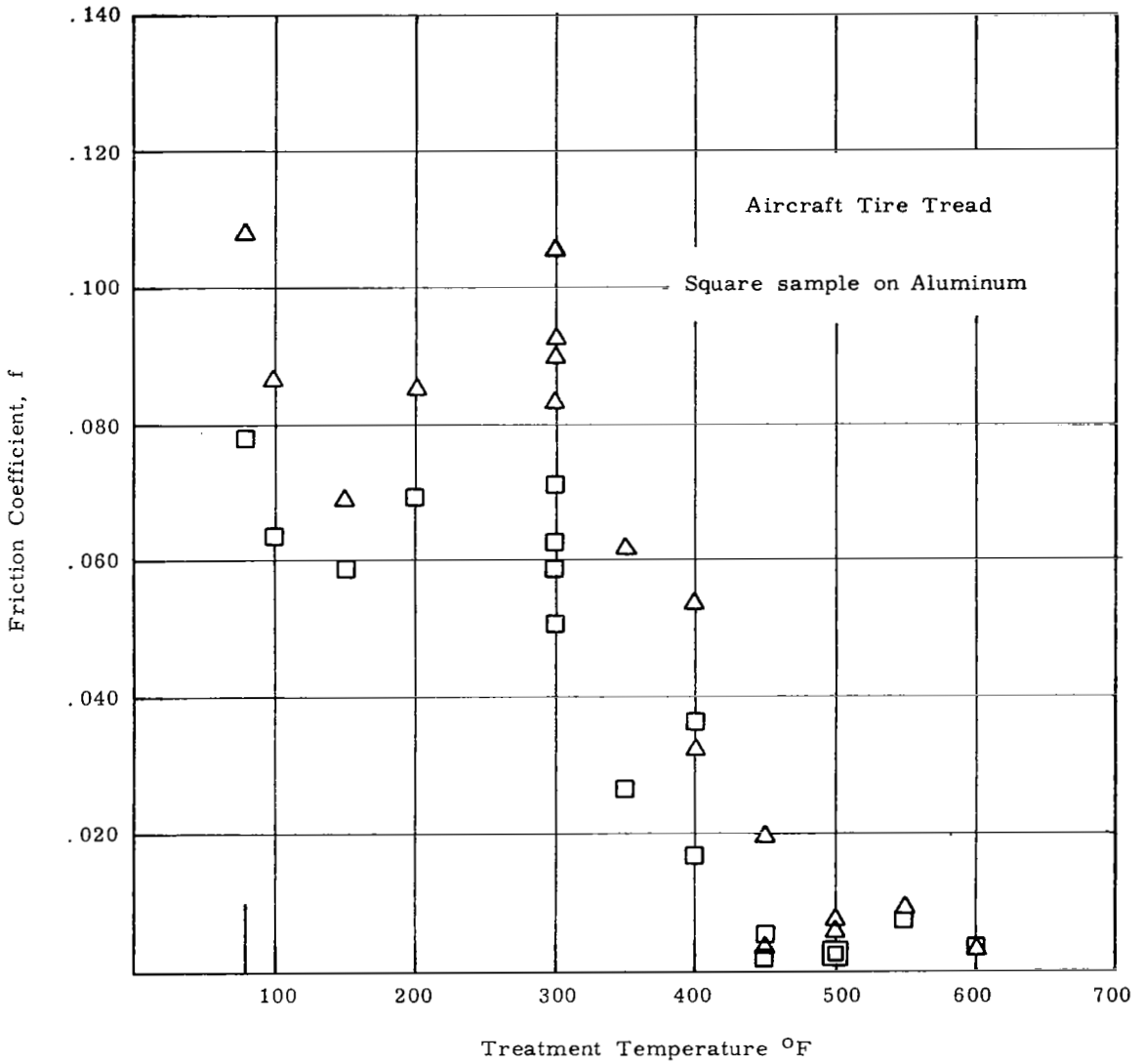

Figure 13. Friction coefficient vs. treatment temperature for aircraft tire tread.

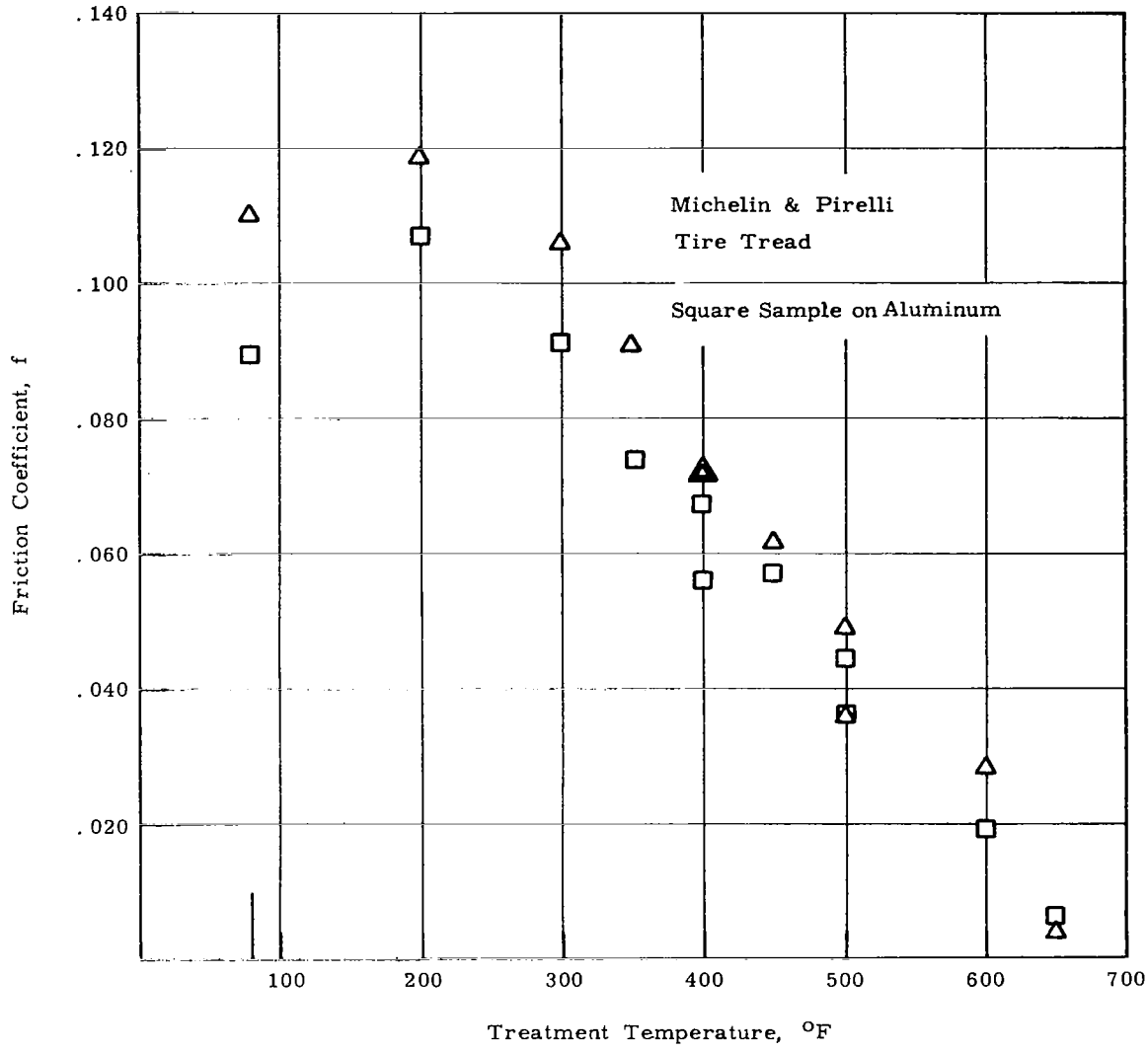

Figure 14. Friction coefficient vs. treatment temperature for Michelin and Pirelli tire tread.

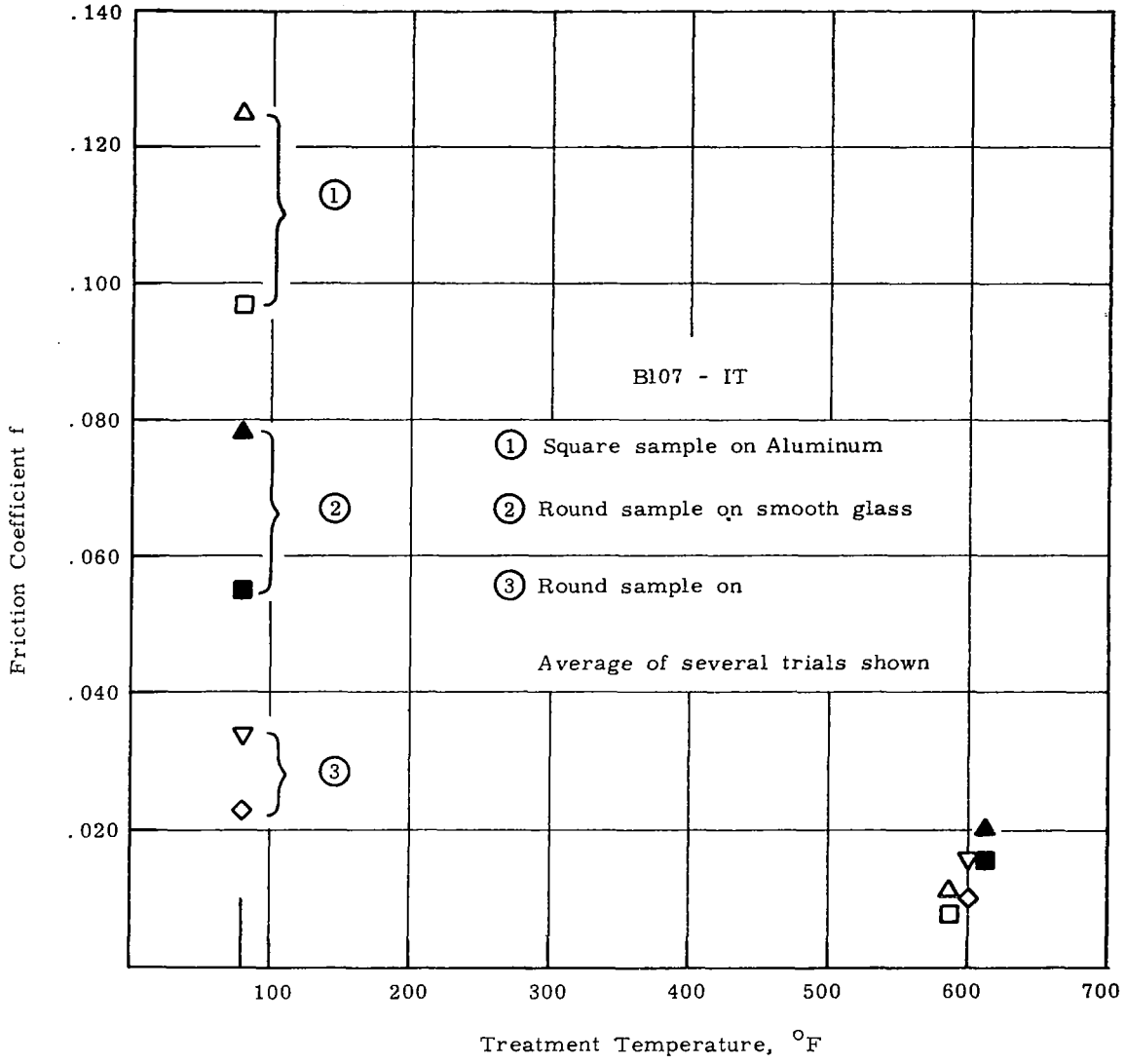

Figure 15. Effect of temperature treatment on friction coefficient.

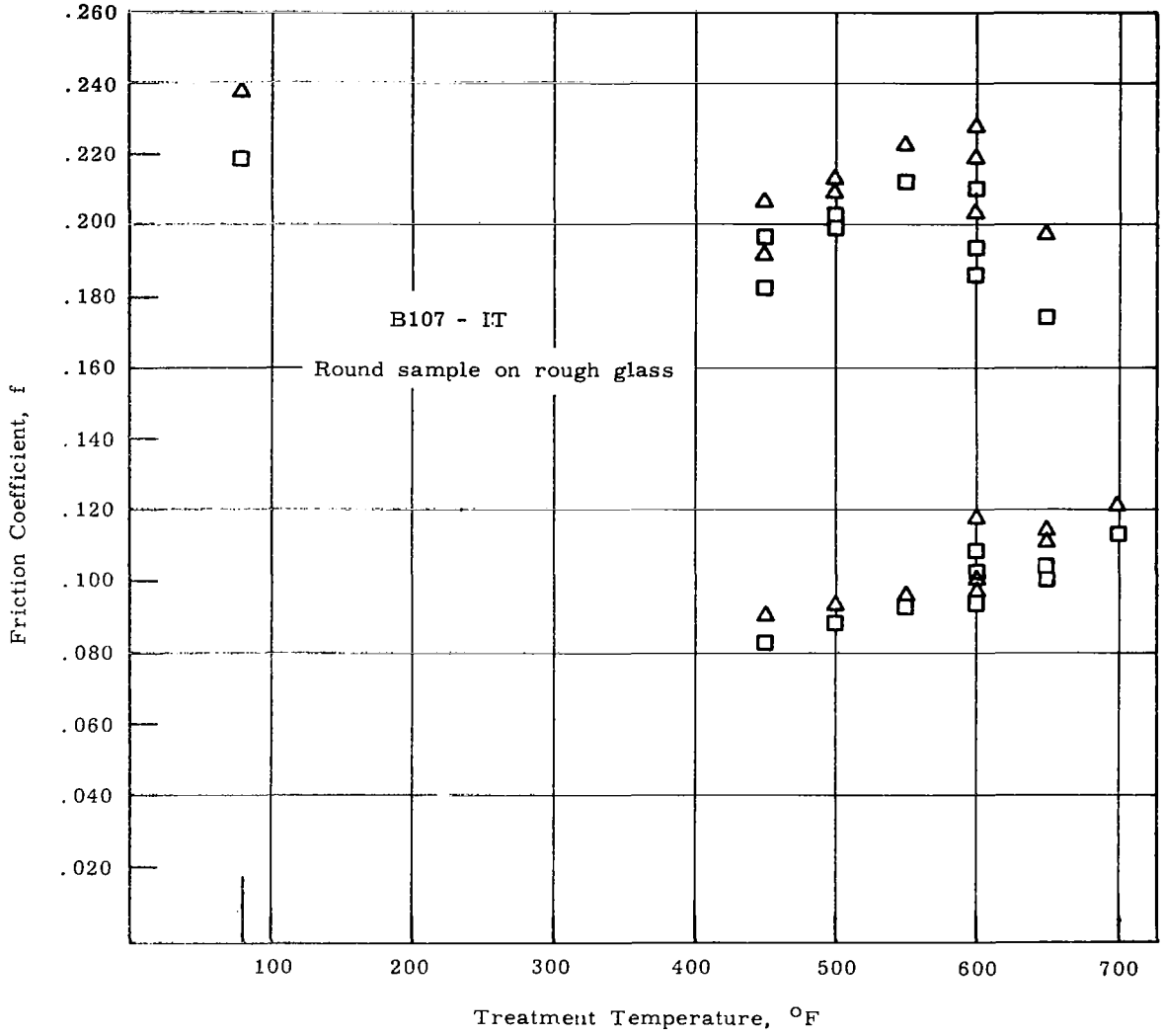

Figure 16. Friction coefficient vs. treatment temperature on rough glass.

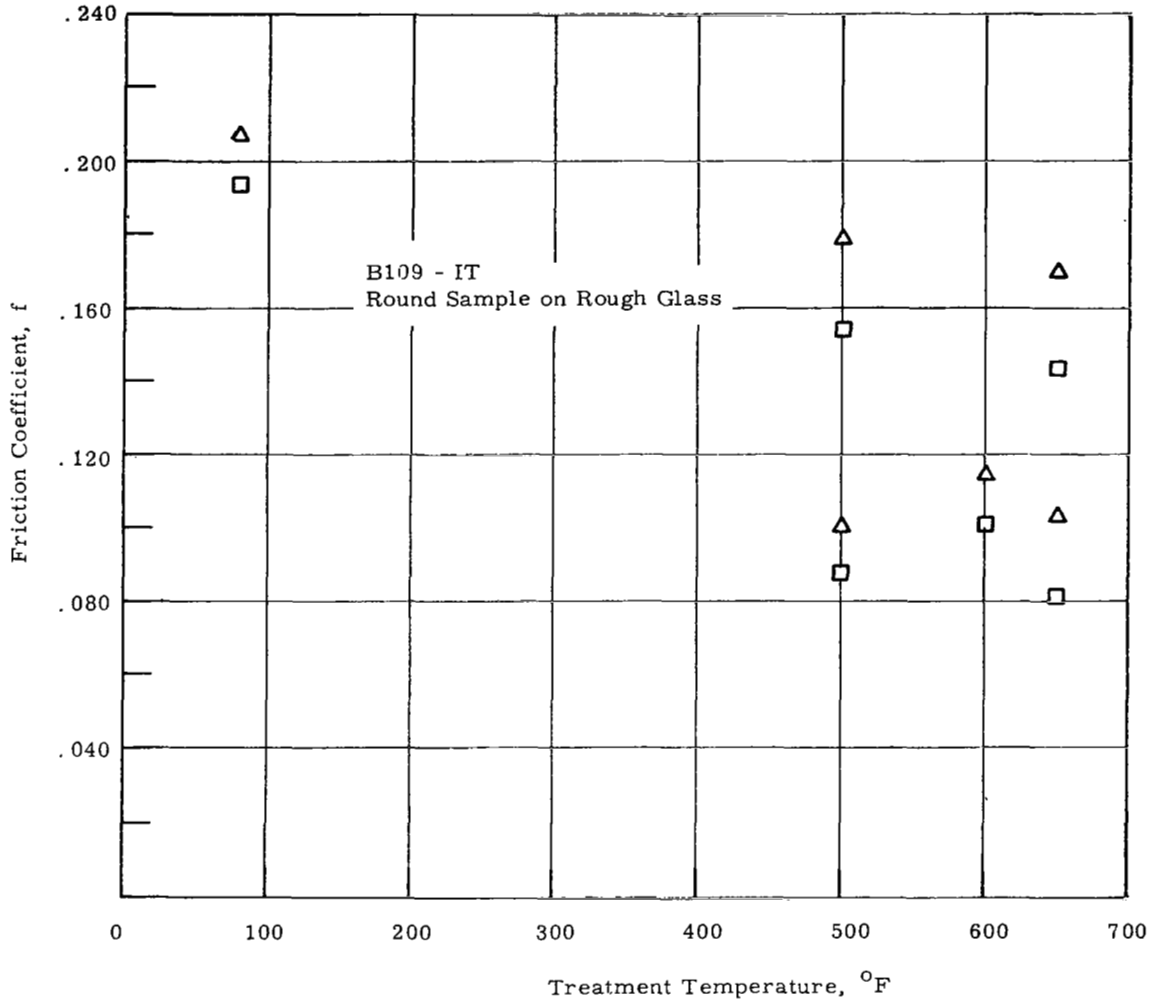

Figure 17. Friction coefficient vs. treatment temperature on rough glass.

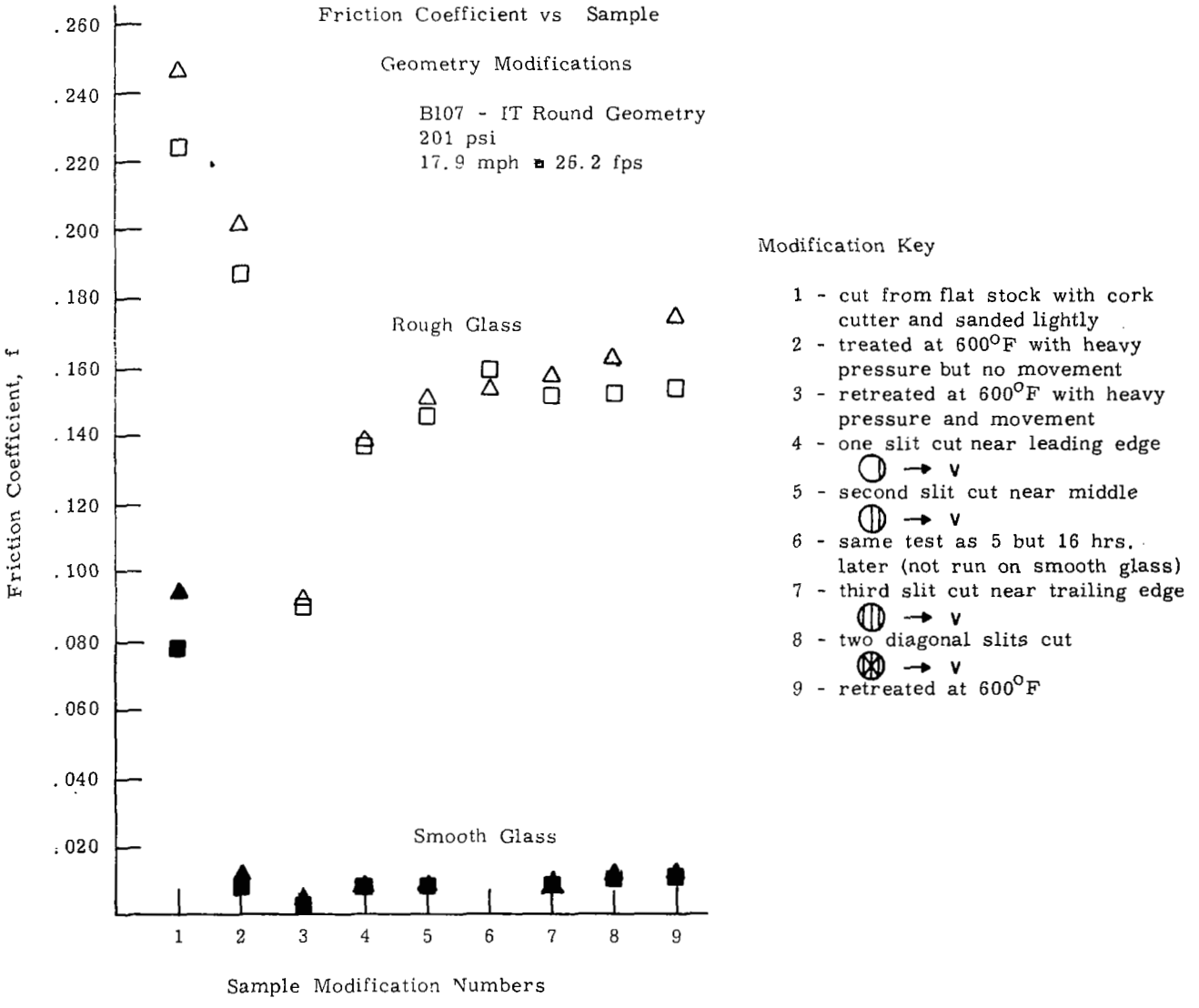

Figure 18. Effect of cuts on friction coefficients of reverted rubber.

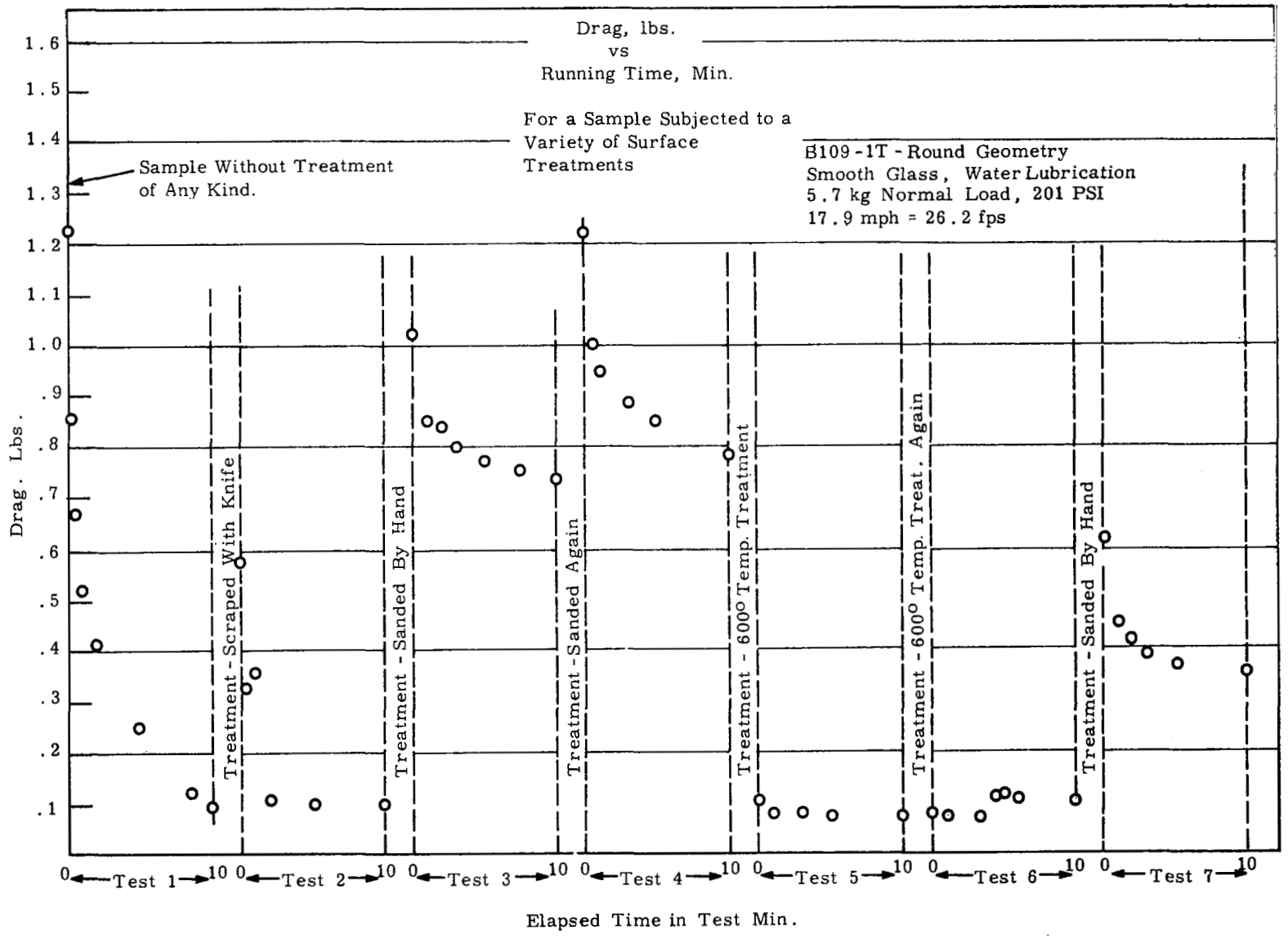

Figure 19. Friction coefficient vs. time and treatment history.

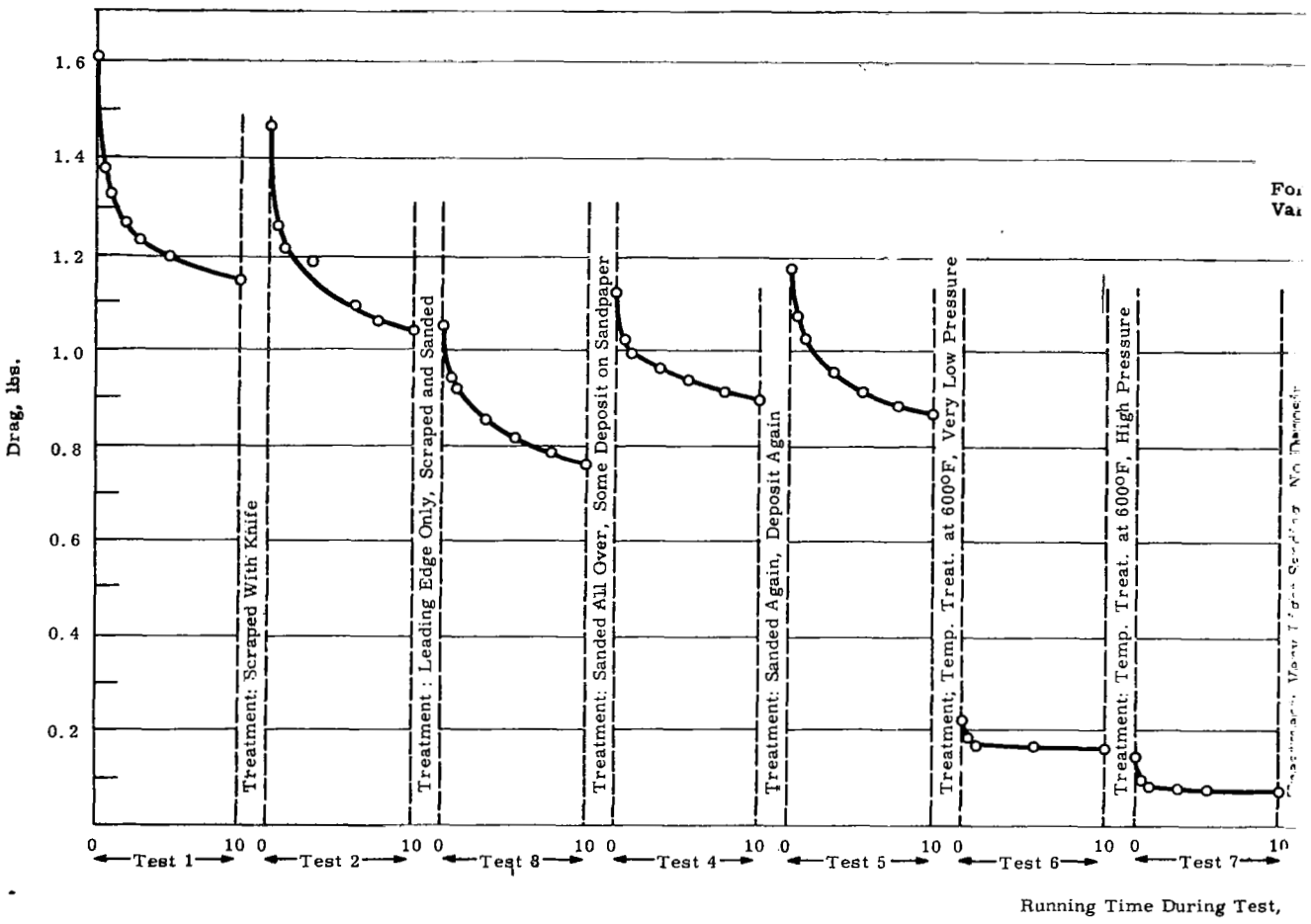

Figure 20. Friction coefficient vs

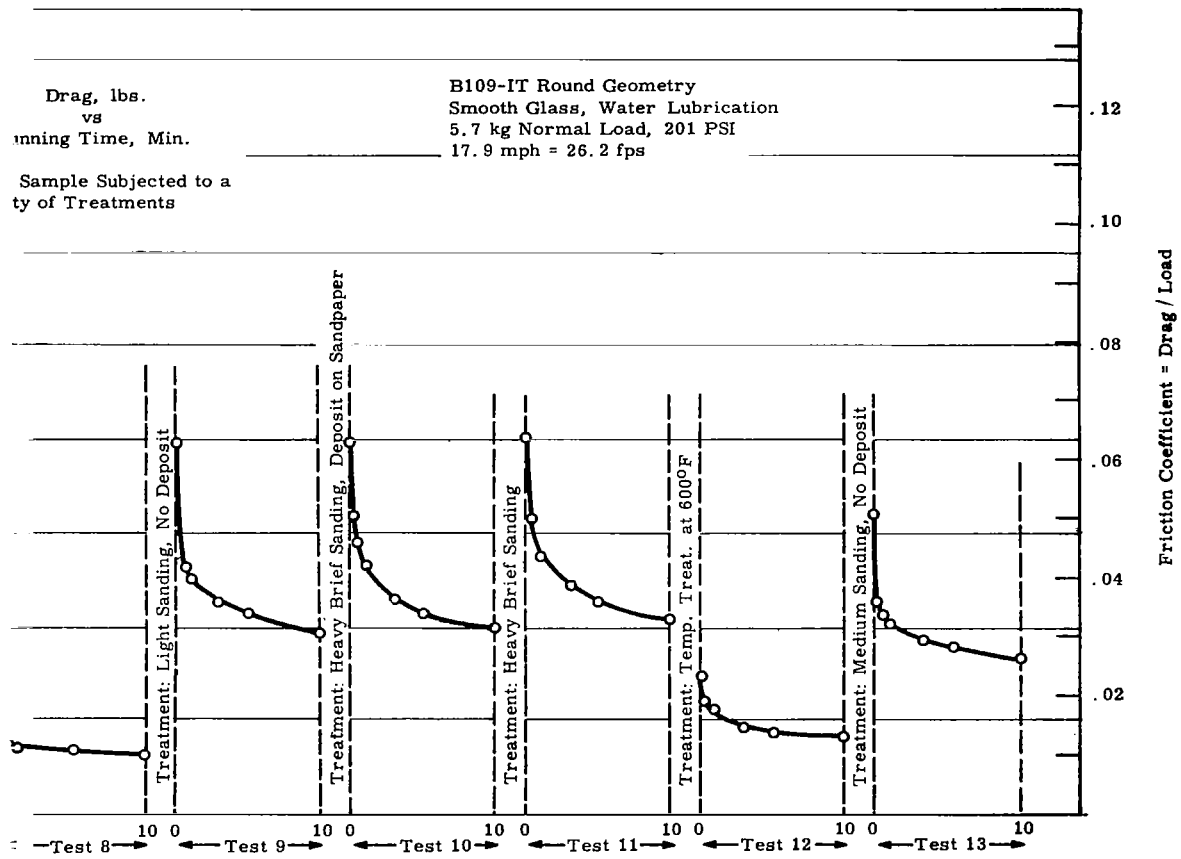

n.

time and treatment history.

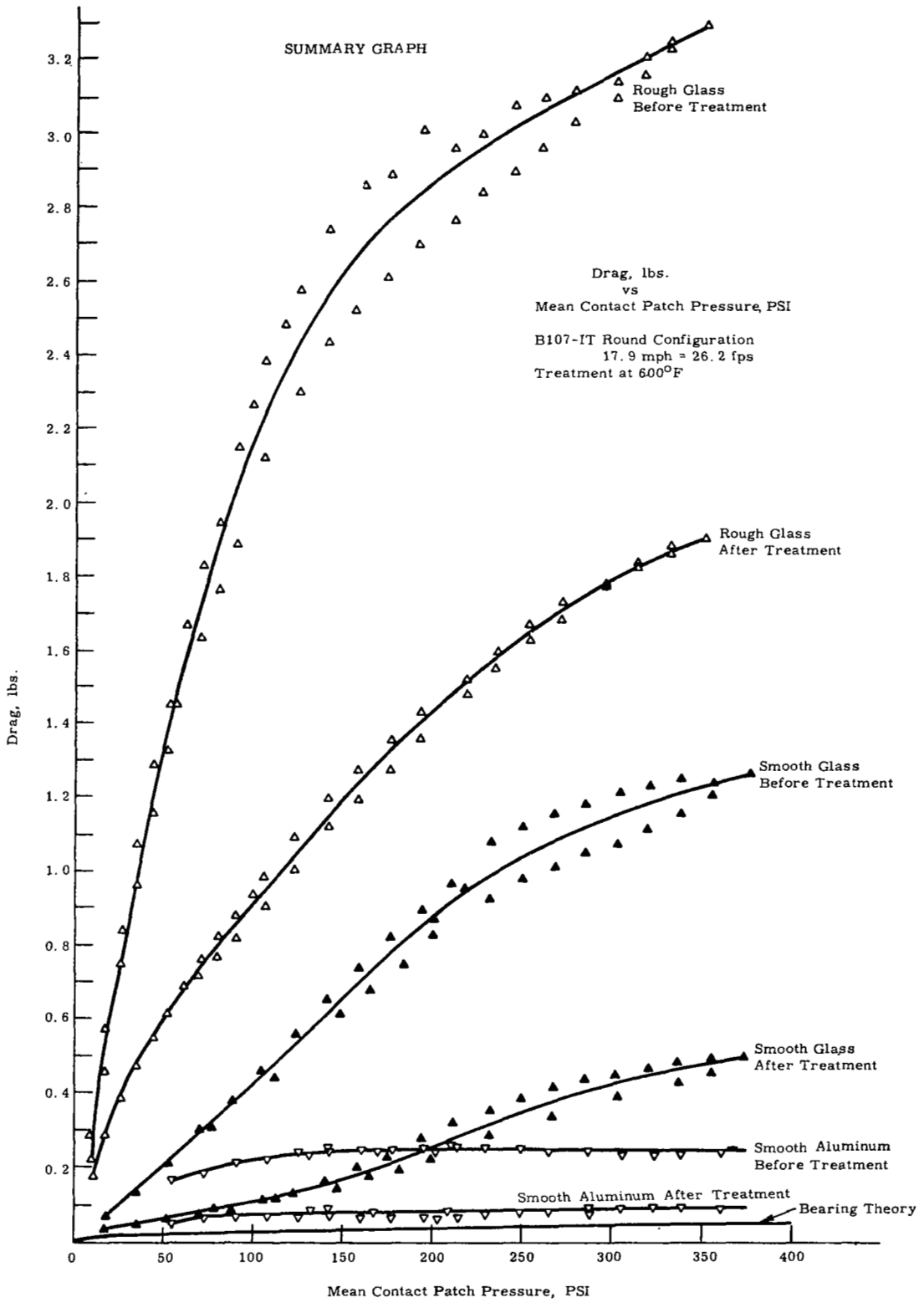

Figure 21. Summary of drag force vs. average contact pressure.

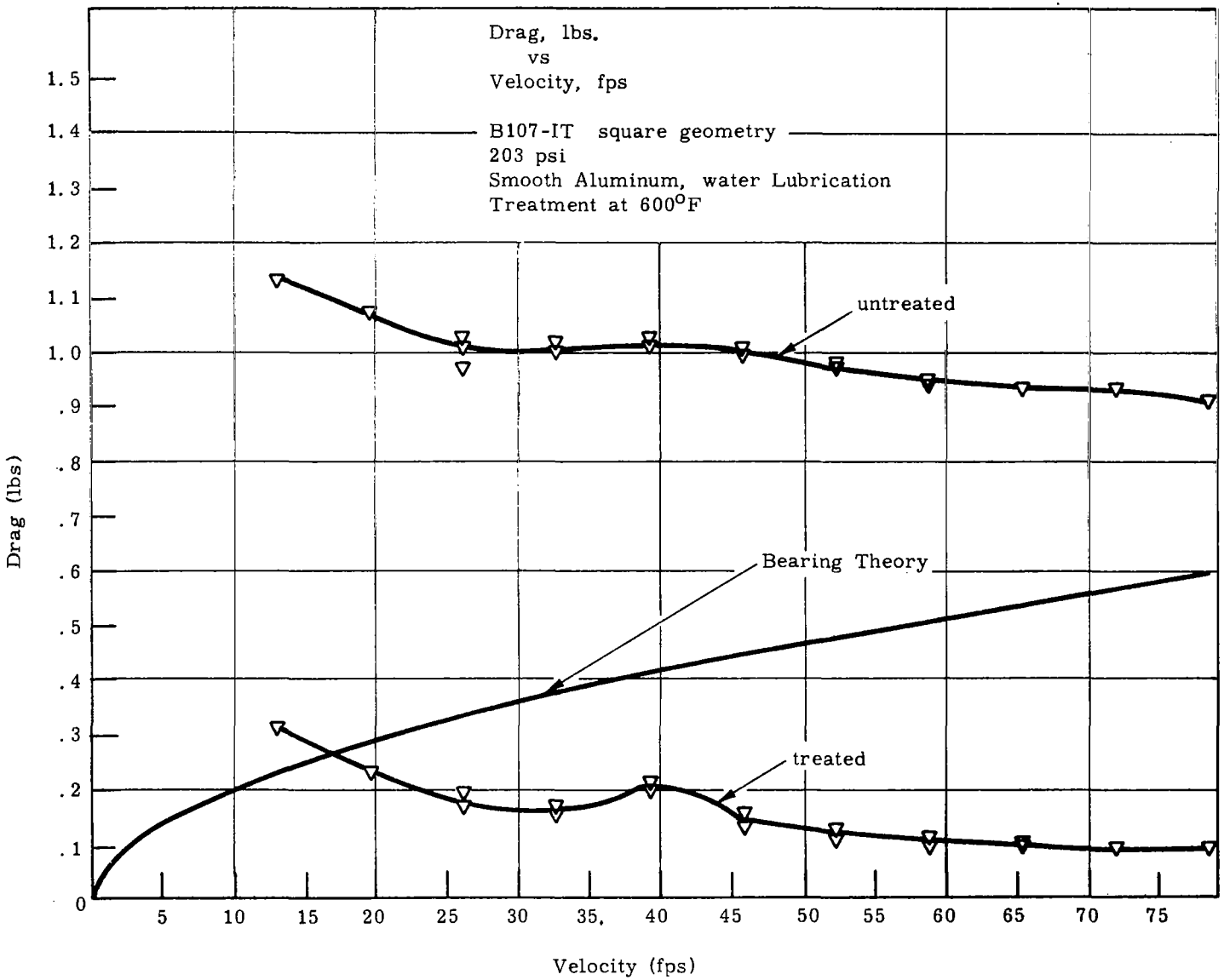

Figure 22. Drag force vs. velocity on an aluminum surface.

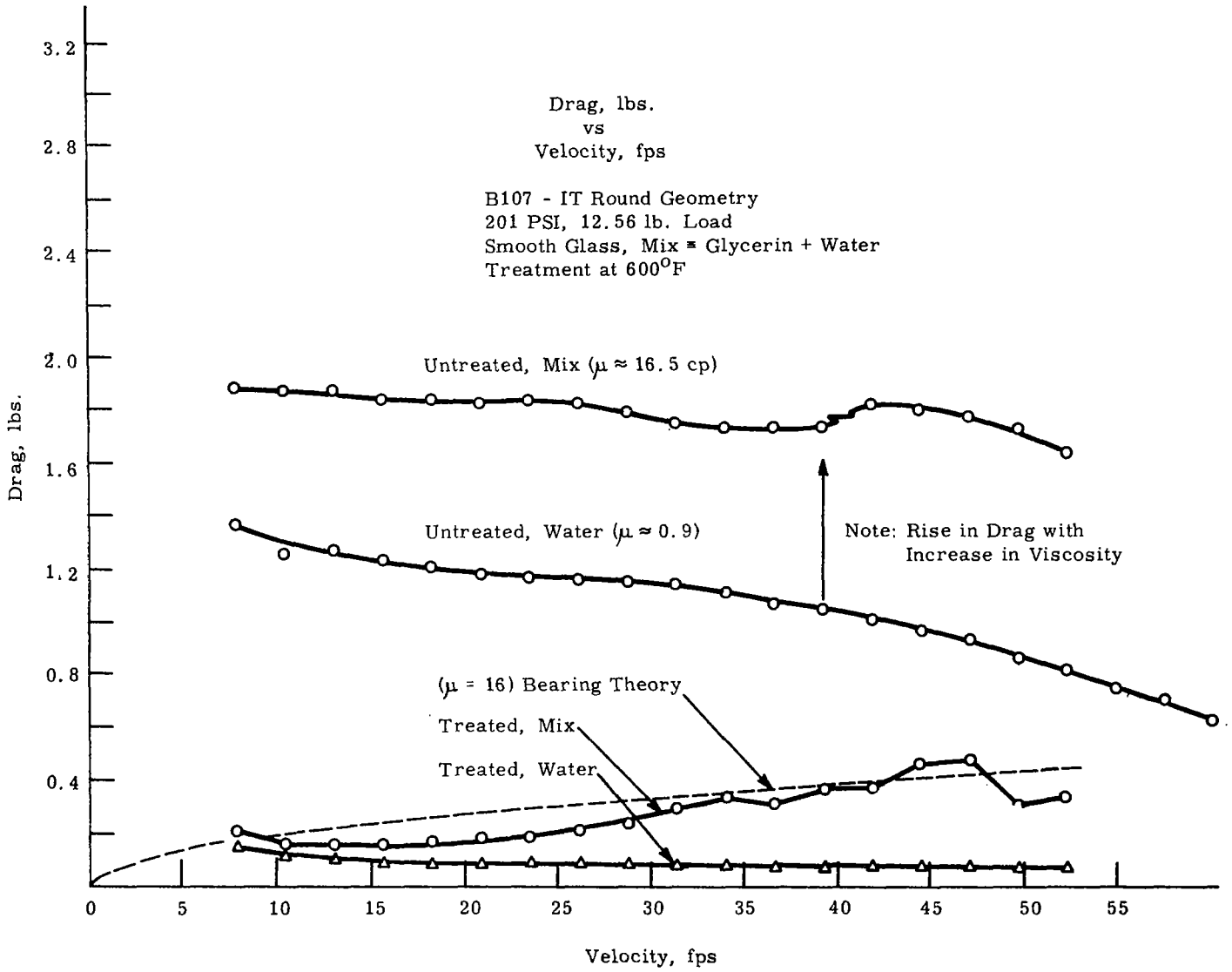

Figure 23. Drag force vs. velocity for several viscosities of water.

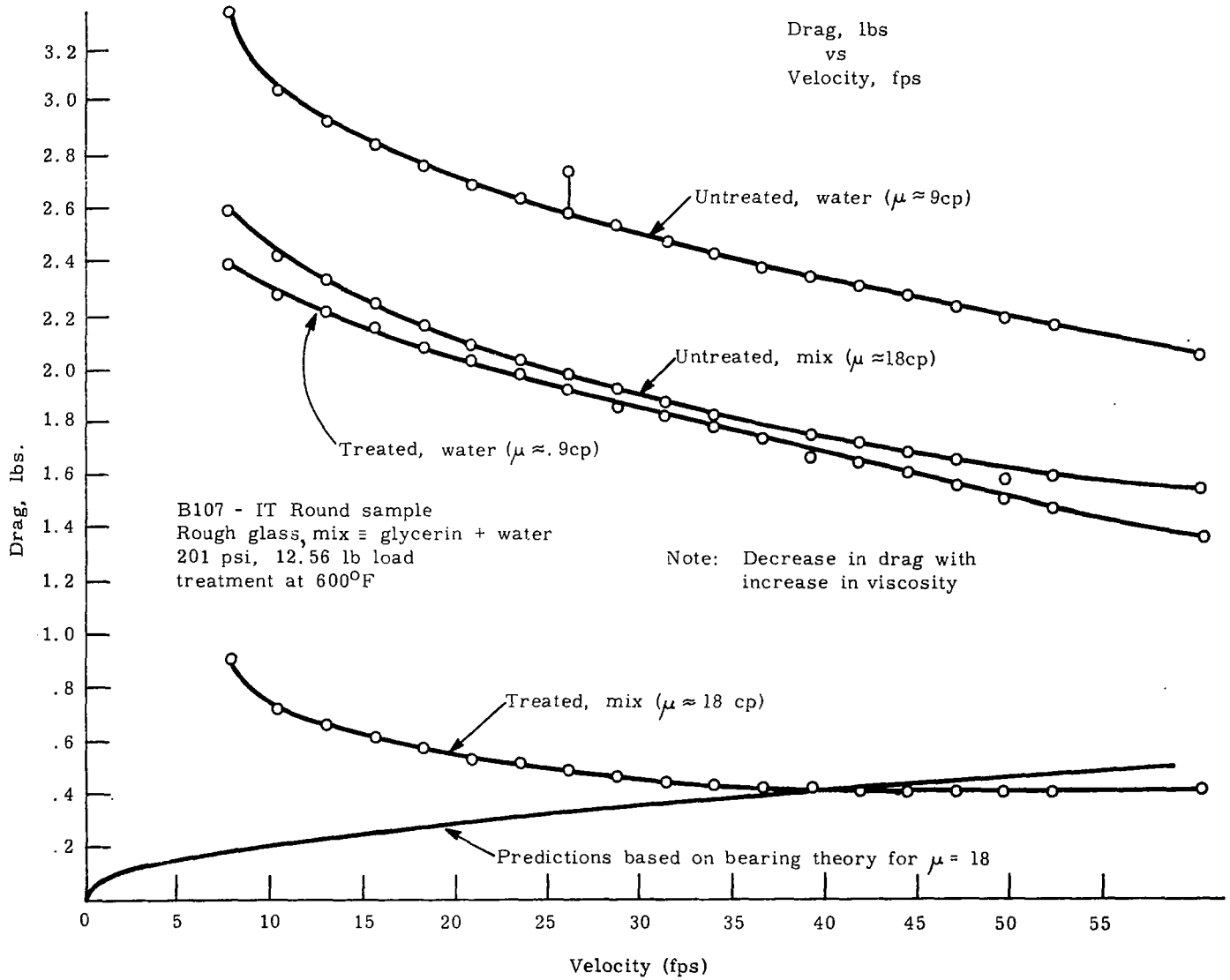

Figure 24. Drag force vs. velocity for several viscosities of water.

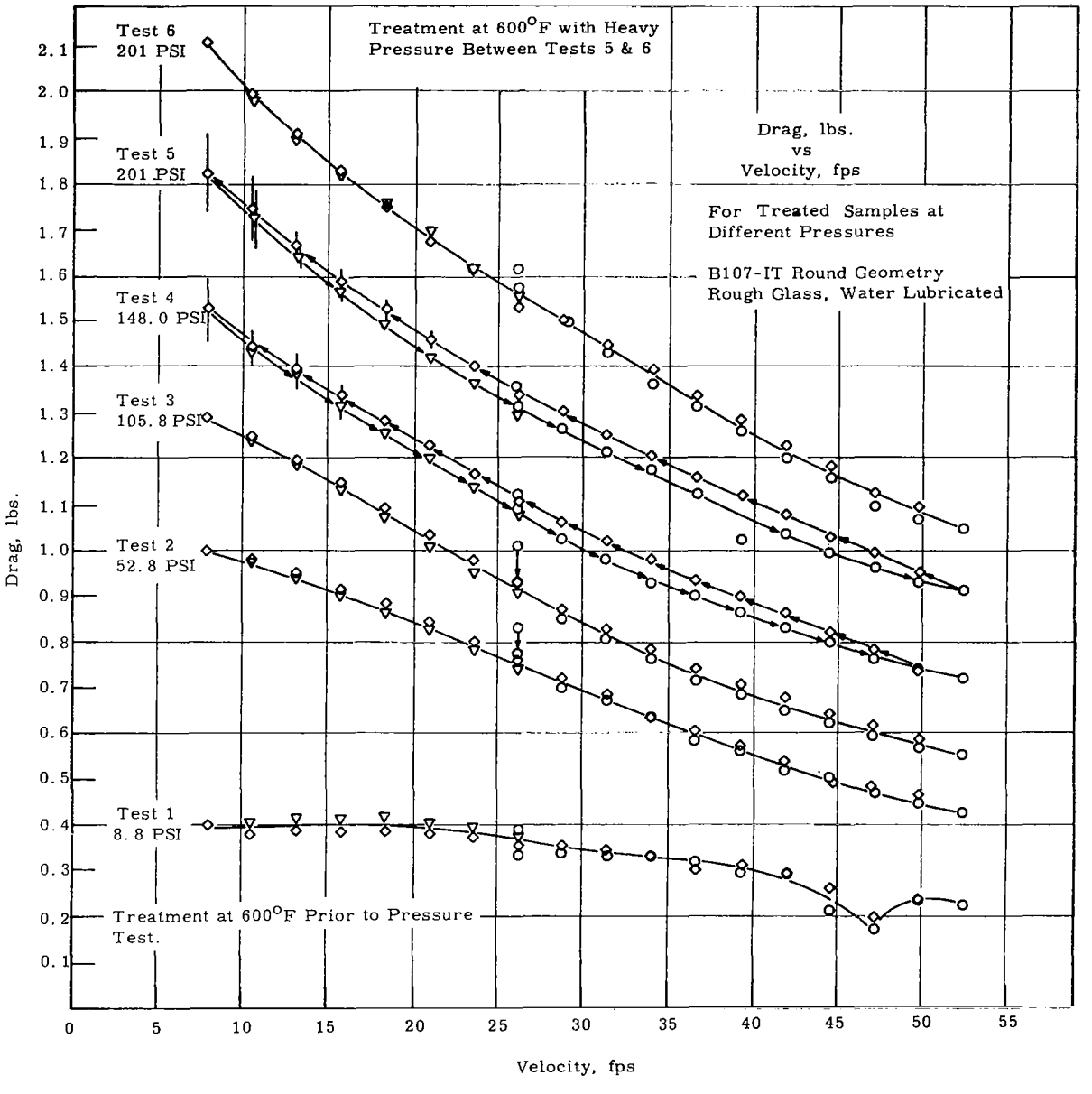

Figure 25. Drag force vs. velocity for several contact pressures.

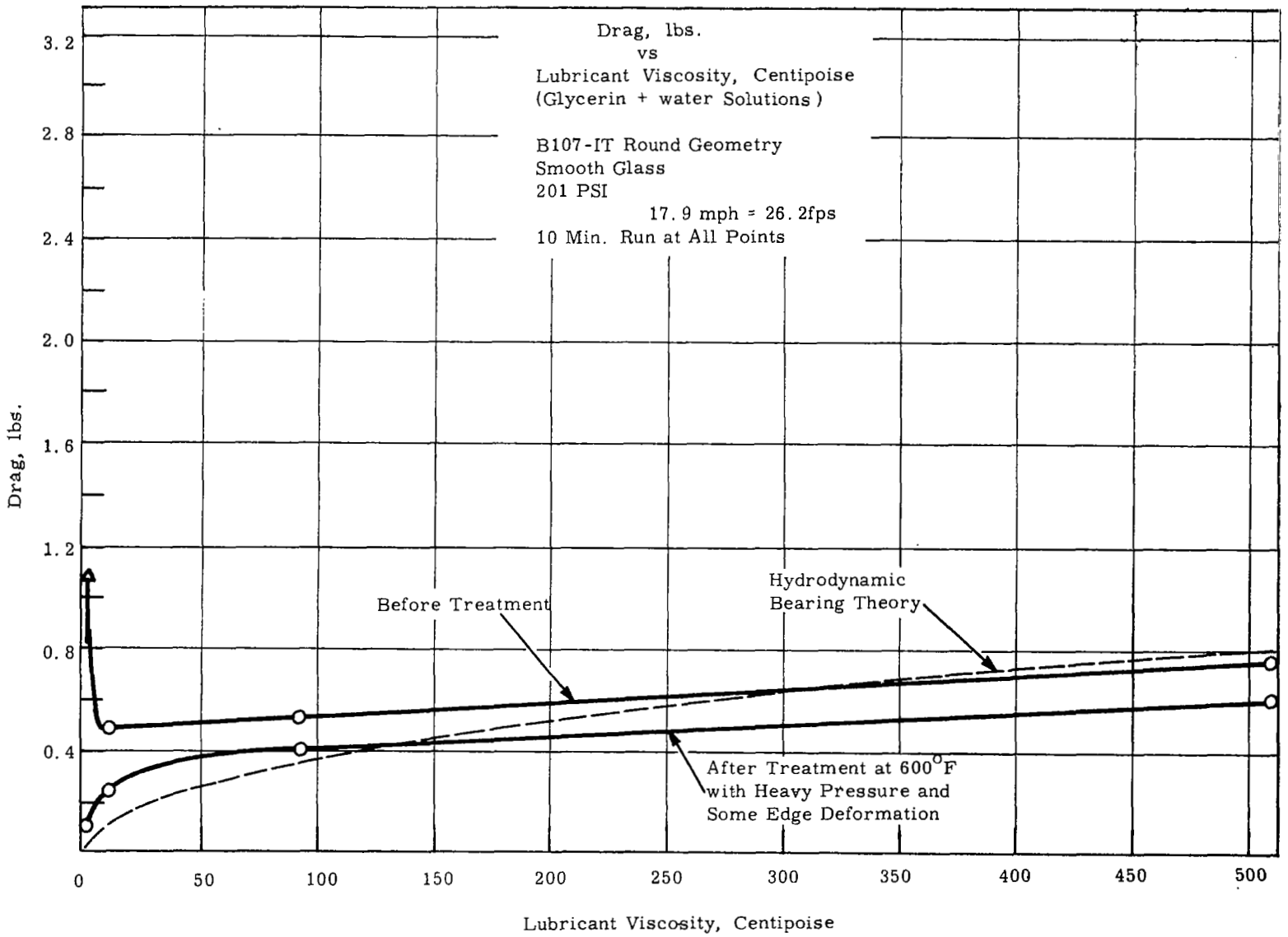

Figure 26. Drag force vs. lubricant viscosity.

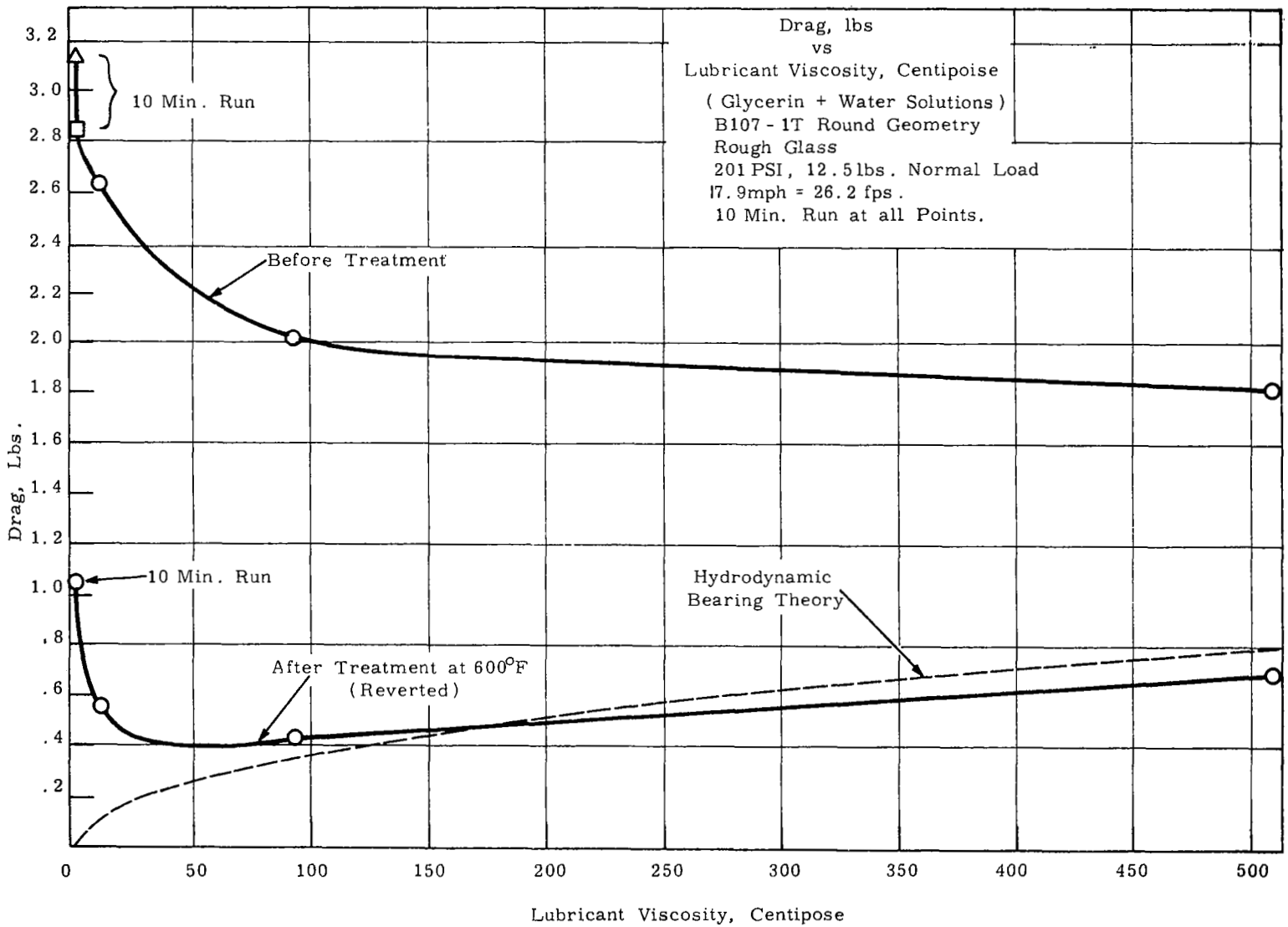

Figure 27. Drag force vs. lubricant viscosity.